The Air Pollution Model (TAPM) Version 2.
Part 2: Summary of Some Verification Studies.

Peter J. Hurley, William L. Physick and Ashok K. Luhar
CSIRO Atmospheric Research
Private Bag 1, Aspendale,
Vic. 3195, Australia

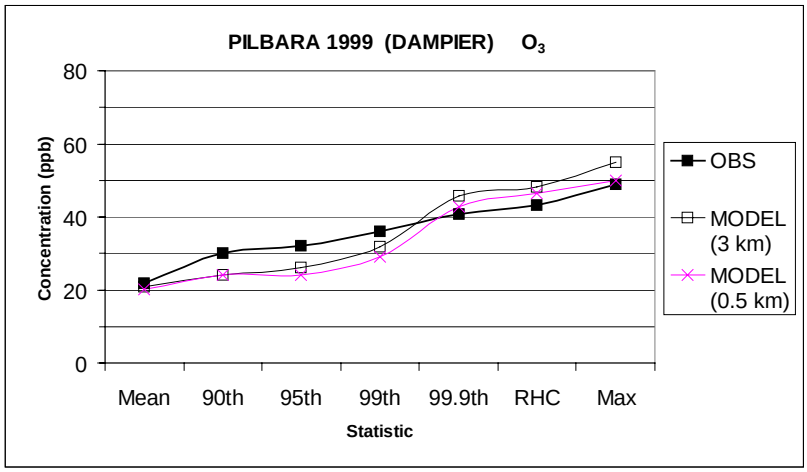

CSIRO
Atmospheric Research

CSIRO Atmospheric Research Technical Paper No.57

The Air Pollution Model (TAPM) Version 2.
Part 2: Summary of Some Verification Studies.

Peter J. Hurley, William L. Physick and Ashok K. Luhar

CSIRO Atmospheric Research Technical Paper No.57

National Library of Australia Cataloguing-in-Publication Entry

Hurley, Peter,
The air pollution model (TAPM) version 2. Part 2, Summary of some verification studies.

ISBN 0 643 06653 5.

1. Air - Pollution - Mathematical models. 2. Air - Pollution - Measurement. 3. Air - Pollution - Meteorological aspects. I. Physick, William Lloyd. II. Luhar, Ashok K. III. CSIRO. Division of Atmospheric Research. IV. Title. (Series : CSIRO Atmospheric Research technical paper ; no. 57).

551.51

Address and contact details: CSIRO Atmospheric Research
Private Bag No 1,
Aspendale Vic 3195
Phone: (+61 3) 9239 4400; fax: (+61 3) 9239 4444
Email: chief@dar.csiro.au

CSIRO Atmospheric Research Technical papers may be issued out of sequence

The Air Pollution Model (TAPM) Version 2. Part 2: Summary of Some Verification Studies.

Peter J. Hurley, William L. Physick and Ashok K. Luhar
CSIRO Atmospheric Research
Private Bag 1, Aspendale,
Vic. 3195, Australia

Abstract

Air pollution predictions for environmental impact assessments usually use Gaussian plume/puff models driven by observationally-based meteorological inputs. An alternative approach is to use prognostic meteorological and air pollution models, which have many advantages over the Gaussian approach and are now becoming a viable tool for performing year-long simulations. Continuing rapid increases in computing power are bringing this approach within reach of a desktop PC. This paper provides some verification studies of The Air Pollution Model (TAPM) for various regions throughout Australia (Cape Grim, Melbourne, Kwinana, Perth and the Pilbara), for two US tracer experiments (Kincaid and Indianapolis) used for international model inter-comparison, and for point source dispersion in wind-tunnel building wakes.

The meteorological results show that TAPM performs well in a variety of regions throughout Australia (e.g., coastal, inland and generally complex terrain for sub-tropical to mid-latitude conditions), including for case studies and year-long simulations. The pollution results show that TAPM performs well for a range of important phenomena (e.g., nocturnal inversion break-up fumigation, convective dispersion, shoreline fumigation, building wakes, and general dispersion in complex rural and urban conditions). In particular, TAPM performs very well for the prediction of extreme pollution statistics, important for environmental impact assessments, for both non-reactive (tracer) and reactive (nitrogen dioxide, ozone and particulate) pollutants for a variety of sources (e.g. industrial stacks and/or general surface or urban emissions).

1 Introduction

Air pollution models that can be used to predict pollution concentrations for periods of up to a year are generally semi-empirical/analytic approaches based on Gaussian plumes or puffs. These models typically use either a simple surface-based meteorological file or a diagnostic wind field model based on available observations. The Air Pollution Model (TAPM) is different to these approaches in that it solves the fundamental fluid dynamics and scalar transport equations to predict meteorology and pollutant concentration for a range of pollutants important for air pollution applications. It consists of coupled prognostic meteorological and air pollution concentration components, eliminating the need to have site-specific meteorological observations. Instead, the model predicts the flows important to local-scale air pollution, such as sea breezes and terrain-induced flows, against a background of larger-scale meteorology provided by synoptic analyses.

This paper follows on from the technical description of the model in part 1 of this series (Hurley, 2002). Sections 2, 3 and 4 summarise some verification studies using TAPM in various regions throughout Australia. These regions include Cape Grim (Hurley, 1999), Melbourne (Hurley, 2000; Hurley *et al*., 2002), Kwinana (Hurley and Luhar 2000; Hurley *et al.*, 2001), Perth (Physick and Cope, 2001; Physick *et al*., 2002a) and the Pilbara (Physick and Blockley, 2001; Physick *et al*. 2002b). In some cases they include a comparison between results from the previous major releases of TAPM (V1.0 and V1.4). TAPM V2.0 is also verified for two US tracer datasets (Kincaid and Indianapolis) used for international model inter-comparison (Section 5), and model performance for a set of standards statistics is compared to a number of other models reported in the literature (Luhar and Hurley, 2002a, 2002b). Finally, TAPM is verified for some wind-tunnel data that simulate point source dispersion in building wakes (Section 6).

2 Comparison of TAPM V1.0, V1.4 and V2.0 for some previous studies

This Section describes simulations performed using TAPM V2.0 and compares these results from some studies done with earlier versions of TAPM (V1.0 and V1.4). The differences between model versions are summarised in the Appendix of part 1 of this series (Hurley, 2002).

2.1 Summer meteorology at Cape Grim

The Cape Grim baseline air monitoring station (144°41.5′E, 40°41′S) is situated on the north-west corner of Tasmania, Australia. The station was set up to measure baseline values of chemicals in the atmosphere, and it also routinely measures winds at 10 m and 50 m above the ground, and temperature and humidity at screen level. The site is situated within a few hundred metres of the coastline both to the west and to the north, with a steep cliff at the coast to the west and a more gradual slope to the north. The station is approximately 95 m above sea level.

TAPM V2.0 was used to model summer meteorology (December 1997 to February 1998) at Cape Grim, using as model input six hourly LAPS analysis data at a grid spacing of 0.75° from the Bureau of Meteorology to provide the synoptic conditions (see Puri *et al*., 1998, for a description of LAPS), Rand's global sea surface temperatures from NCAR, 9-second DEM terrain height data from AUSLIG, and soil and vegetation classification data from CSIRO Wildlife and Ecology. The model was run with a triply nested grid of 25 × 25 × 20 points at 10,000-m, 3,000-m and 1,000-m horizontal grid spacing, with default model options and a deep soil moisture content of 0.05 (very dry), which is close to the wilting value for grassland on the sandy soil that dominates the area.

Table 2.1: Statistics for TAPM V2.0 simulation of Summer 1997-98 at Cape Grim for wind speed at 10 and 50 m above the ground (WS10, WS50); the west-east-component of the wind (U10, U50); the south-north-component of the wind (V10, V50); temperature (TEMP); and relative humidity (RH).

VARIABLE	NUMBER	MEAN_OBS	MEAN_MOD	STD_OBS	STD_MOD	CORR	RMSE	RMSE_S	RMSE_U	IOA	SKILL_E	SKILL_V	SKILL_R
WS10	2160	9.4	6.4	4.6	2.8	0.76	4.31	3.90	1.83	0.71	0.40	0.62	0.95
U10	2160	3.8	3.3	7.8	4.7	0.90	4.13	3.60	2.03	0.89	0.26	0.60	0.53
V10	2160	2.7	1.2	5.1	3.7	0.77	3.64	2.75	2.38	0.82	0.46	0.73	0.71
WS50	1298	9.3	7.8	4.3	3.5	0.80	2.94	2.08	2.08	0.85	0.49	0.82	0.69
U50	1298	3.8	4.3	7.1	5.8	0.92	2.98	1.86	2.33	0.94	0.33	0.81	0.42
V50	1298	2.7	1.4	5.7	4.4	0.84	3.35	2.34	2.40	0.89	0.42	0.78	0.59
TEMP	2158	14.8	15.1	2.3	2.5	0.86	1.30	0.35	1.25	0.92	0.55	1.07	0.57
RH	2160	76.1	77.8	10.4	11.1	0.49	11.06	5.29	9.71	0.70	0.93	1.07	1.06

KEY: OBS = Observations, MOD = Model Predictions, NUMBER = Number of hourly-averaged values used for the statistics, MEAN = Arithmetic mean, STD = Standard Deviation, CORR = Pearson Correlation Coefficient (0 = no correlation, 1 = exact correlation), RMSE = Root Mean Square Error, RMSE_S = Systematic Root Mean Square Error, RMSE_U = Unsystematic Root Mean Square Error, IOA = Index of Agreement (0 = no agreement, 1 = perfect agreement), SKILL_E = (RMSE_U)/(STD_OBS) (<1 shows skill), SKILL_V = (STD_MOD)/(STD_OBS) (near to 1 shows skill), SKILL_R = (RMSE)/(STD_OBS) (<1 shows skill).

Model predictions were extracted at the nearest grid point to the Cape Grim site on the inner grid (1,000-m spacing) at the lowest two model levels (10 m and 50 m above the ground) for winds and at screen-level for temperature. Statistics of observations and model predictions are shown in Table 2.1. The statistics used were based on the recommendations of Willmott (1981), as described in the Appendix, and include the Index Of Agreement (IOA) that provides a more consistent measure of performance than the correlation coefficient (also shown for comparison). The IOA is a measure of how well predicted variations about the observed mean are represented, with a value greater than about 0.50 considered to be good, as judged by several other published prognostic modelling studies (see Hurley, 2000).

Based on the IOA and the Skill Score statistics, the results suggest that temperature and 50-m level winds are predicted the best, while 10-m level wind speed and relative humidity are predicted less accurately. At 10 m, the mean wind speed was underestimated and the systematic component of the RMSE dominates the unsystematic component. This is perhaps not surprising given the complexity of the local-scale topography at Cape Grim, which can lead to complex flow behaviour that the model (even at 1,000-m grid resolution) does not resolve. Baines and Murray (1991) illustrated this point with physical modelling of the flow behaviour at Cape Grim. They showed that under westerly synoptic winds the air reaching the measurement levels at the site were from a height of approximately 50 m higher upwind over the sea, so that the 50-m level on the tower was measuring air that had come from a height of 100 m. Given the influence that the small-scale terrain effects have on the measurements, the model has performed well in predicting the observed meteorology in the Cape Grim region.

Comparing the TAPM V2.0 results with predictions from previous release versions of TAPM (V1.0 and V1.4) shows that the results have improved with the latest release of the model (see Hurley, 1999, for TAPM V1.0 results). This can be seen when examining the RMSE and IOA values from the various model versions. For winds at 50 m (averaged over wind speed and the wind components), the

- RMSE values for V1.0, V1.4 and V2.0 are 3.7, 3.3 and 3.1 m s^{-1} respectively;
- IOA values for V1.0, V1.4 and V2.0 are 0.83, 0.89 and 0.89 respectively.

For temperature, the

- RMSE values for V1.0, V1.4 and V2.0 are 1.4, 1.8 and 1.3ºC respectively;
- IOA values for V1.0, V1.4 and V2.0 are 0.84, 0.81 and 0.92 respectively.

2.2 Urban winter and summer meteorology in Melbourne

Melbourne (144°53′E, 37°49′S) is a coastal city in the southern part of Victoria, Australia, with ocean to the south and mountains to the north. EPA Victoria operates an air monitoring network covering the urban region of Melbourne and Geelong, and measures both near-surface meteorology and air pollution (see Figure 2.1).

TAPM V2.0 was used to model winter (July 1998) and summer (December 1998) meteorology in Melbourne, using as model input six hourly LAPS analysis data at a grid spacing of 0.75° from the Bureau of Meteorology to provide the synoptic conditions (see Puri *et al*., 1998, for a description of LAPS), Rand's global sea surface temperatures from NCAR, 9-second DEM terrain height data from AUSLIG, and soil and vegetation classification data from CSIRO Wildlife and Ecology. The model was run with nested grids of 40 × 40 × 20 points at 30,000-m, 10,000-m and 3,000-m spacing, with default model options and a deep soil moisture content of 0.20 (moist) for winter and 0.10 (dry) for summer. Land-use was dominated by urban characteristics for most of the twelve sites in the monitoring network.

More detail on the Melbourne region, can be found in Hurley (2000), which also presents TAPM V1.0 results.

Model predictions were extracted at the nearest grid point to each of the eleven monitoring sites on the inner grid (3,000-m spacing) at the lowest model level (10 m above the ground) for winds and at screen-level for temperature. Statistics of observations and model predictions are shown in Table 2.2 for winter and Table 2.3 for summer. The statistics used were based on the recommendations of Willmott (1981), as described in the Appendix. The results suggest that both winds and temperature are predicted very well, with no significant biases, low RMSE and high IOA, even though winter temperature variation is much lower than for summer.

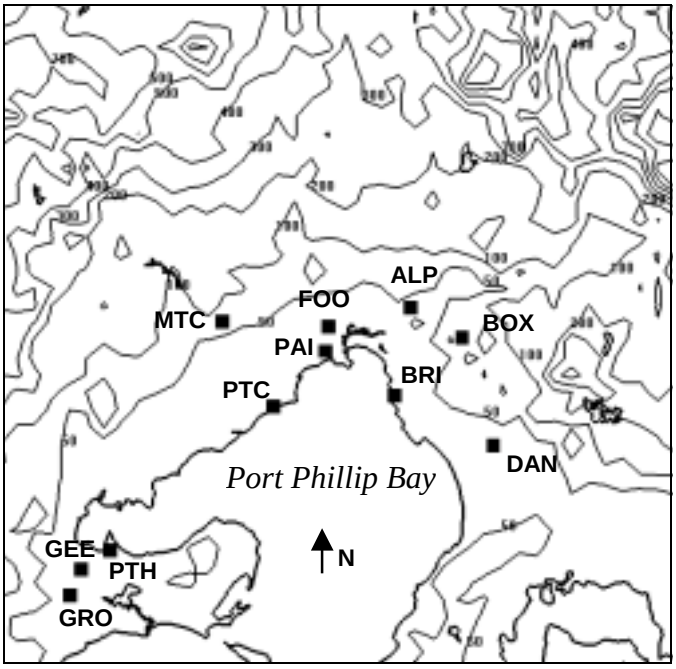

Figure 2.1. Melbourne inner grid domain at 3,000-m resolution with a west-east and south-north extent of 117 km. A detailed coastline and marked terrain height (m) contours are shown. The EPAV monitoring sites are marked, and correspond to: Alphington (ALP), Box Hill (BOX), Brighton (BRI), Dandenong (DAN), Footscray (FOO), Geelong South (GEE), Grovedale (GRO), Mt. Cottrell (MTC), Paisley (PAI), Pt. Cook (PTC) and Pt. Henry (PTH).

Comparing the TAPM V2.0 results with predictions from previous release versions of TAPM (V1.0 and V1.4) shows that the winter results have improved with the latest release of the model – results from TAPM V1.0 are described in more detail in Hurley (2000). This can be seen when examining the RMSE and IOA values from the various model versions. For winds at 10 m (averaged over wind speed and the wind components), the

- RMSE values for V1.0, V1.4 and V2.0 are 1.7, 2.1 and 1.6 m s^{-1} respectively;
- IOA values for V1.0, V1.4 and V2.0 are 0.82, 0.82 and 0.87 respectively.

For temperature, the

- RMSE values for V1.0, V1.4 and V2.0 are 3.4, 2.8 and 2.5ºC respectively;
- IOA values for V1.0, V1.4 and V2.0 are 0.78, 0.79 and 0.84 respectively.

Table 2.2. Statistics for TAPM V2.0 simulation of July 1998 in Melbourne (averaged over 11 sites) for wind speed at 10 m above the ground (WS10); the west-east-component of the wind (U10); the south-north-component of the wind (V10); and temperature (TEMP).

VARIABLE	NUMBER	MEAN_OBS	MEAN_MOD	STD_OBS	STD_MOD	CORR	RMSE	RMSE_S	RMSE_U	IOA	SKILL_E	SKILL_V	SKILL_R
WS10	716	3.1	3.6	2.2	2.1	0.82	1.41	0.71	1.21	0.89	0.57	1.00	0.66
U10	716	1.3	1.6	2.3	2.3	0.74	1.69	0.72	1.52	0.85	0.70	1.05	0.78
V10	716	-1.3	-1.1	2.3	2.9	0.79	1.79	0.44	1.72	0.87	0.75	1.24	0.78
TEMP	740	8.9	9.5	3.1	3.4	0.75	2.52	1.03	2.21	0.84	0.73	1.10	0.82

KEY: OBS = Observations, MOD = Model Predictions, NUMBER = Number of hourly-averaged values used for the statistics, MEAN = Arithmetic mean, STD = Standard Deviation, CORR = Pearson Correlation Coefficient (0 = no correlation, 1 = exact correlation), RMSE = Root Mean Square Error, RMSE_S = Systematic Root Mean Square Error, RMSE_U = Unsystematic Root Mean Square Error, IOA = Index of Agreement (0 = no agreement, 1 = perfect agreement), SKILL_E = (RMSE_U)/(STD_OBS) (<1 shows skill), SKILL_V = (STD_MOD)/(STD_OBS) (near to 1 shows skill), SKILL_R = (RMSE)/(STD_OBS) (<1 shows skill).

Comparing the TAPM V2.0 results with predictions from previous release versions of TAPM (V1.0 and V1.4) shows that the summer results have improved with the latest release of the model – results from TAPM V1.0 are described in more detail in Hurley (2000). This can be seen when examining the RMSE and IOA values from the various model versions. For winds at 10 m (averaged over wind speed and the wind components), the

- RMSE values for V1.0, V1.4 and V2.0 are 2.2, 2.2 and 1.8 m s^{-1} respectively;
- IOA values for V1.0, V1.4 and V2.0 are 0.79, 0.81 and 0.87 respectively.

For temperature, the

- RMSE values for V1.0, V1.4 and V2.0 are 3.9, 3.0 and 2.8ºC respectively;
- IOA values for V1.0, V1.4 and V2.0 are 0.90, 0.93 and 0.95 respectively.

Table 2.3. Statistics for TAPM V2.0 simulation of December 1998 in Melbourne (averaged over 11 sites) for wind speed at 10 m above the ground (WS10); the west-east-component of the wind (U10); the south-north-component of the wind (V10); and temperature (TEMP).

VARIABLE	NUMBER	MEAN_OBS	MEAN_MOD	STD_OBS	STD_MOD	CORR	RMSE	RMSE_S	RMSE_U	IOA	SKILL_E	SKILL_V	SKILL_R
WS10	694	4.1	4.0	2.2	2.1	0.71	1.69	0.88	1.43	0.82	0.68	0.97	0.80
U10	694	0.7	0.9	3.1	2.8	0.84	1.74	0.77	1.52	0.90	0.51	0.93	0.58
V10	694	1.6	1.0	3.0	3.1	0.80	2.07	0.79	1.87	0.88	0.65	1.09	0.71
TEMP	717	18.6	18.5	6.0	6.9	0.92	2.82	0.72	2.72	0.95	0.46	1.16	0.48

KEY: OBS = Observations, MOD = Model Predictions, NUMBER = Number of hourly-averaged values used for the statistics, MEAN = Arithmetic mean, STD = Standard Deviation, CORR = Pearson Correlation Coefficient (0 = no correlation, 1 = exact correlation), RMSE = Root Mean Square Error, RMSE_S = Systematic Root Mean Square Error, RMSE_U = Unsystematic Root Mean Square Error, IOA = Index of Agreement (0 = no agreement, 1 = perfect agreement), SKILL_E = (RMSE_U)/(STD_OBS) (<1 shows skill), SKILL_V = (STD_MOD)/(STD_OBS) (near to 1 shows skill), SKILL_R = (RMSE)/(STD_OBS) (<1 shows skill).

2.3 Year-long meteorology and air pollution in the Kwinana industrial region

Kwinana (115°46.5′E, 32°11.5'S) is a major heavy industrial area 30 km south of Perth, Western Australia. It is a coastal area with sea to the west (Indian Ocean) and land to the east, an approximately north-south coastline, and relatively flat local terrain (see Figure 2.2). The Kwinana region includes industries such as power generation, refineries (oil, alumina and nickel), iron smelting, cement works, and titanium dioxide and fertilizer plants. Most of the twenty point sources are on the coast, and they have plume heights that vary from tens of metres up to a few hundred metres. The plumes generally fumigate to ground in the strong south-westerly sea-breeze flow, resulting in relatively high concentrations at distances of up to several kilometres from the coast. The regulatory framework in the region, controlled by the Department of Environmental and Water Catchment Protection (DEWCP), is a model-based control policy that uses the air quality model DISPMOD to relate ground-level concentrations back to emissions (Rayner, 1998). The Kwinana Industries Council (KIC) was established in the course of Policy development to provide a forum for negotiations between industries and to form a single body to represent industry's viewpoint. The strong regulatory framework, and government and industry cooperation, have produced a high quality hour-by-hour emissions inventory for the industrial sources in the region. The Kwinana air monitoring network, measuring both near-surface meteorology and air pollution, was designed to capture the maximum ground level concentrations outside of the industrial zone boundaries, and near local towns, under sea-breeze fumigation conditions. The detailed emission inventory, coupled with the extensive monitoring network data, provide an excellent framework for model development and/or verification.

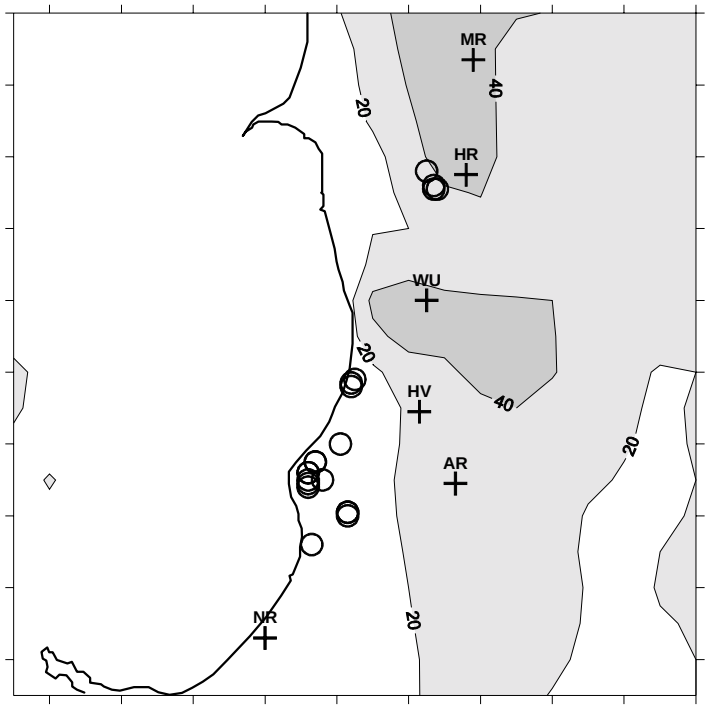

Figure 2.2. TAPM inner grid pollution domain for the Kwinana region with a west-east and south-north extent of 19 km. A detailed coastline and marked terrain height (m) contours with shading for higher heights are shown. The sources are shown as circles (O). The monitoring sites (+) correspond to: North Rockingham (NR), Abercrombie Road (AR), Hope Valley (HV), Wattleup (WU), Henderson Road (HR) and Miguel Road (MR).

TAPM was used to model 1997 meteorology in Kwinana, using as model input six-hourly LAPS analysis data at a grid spacing of 0.75° from the Bureau of Meteorology to provide the synoptic conditions (see Puri *et al*., 1998, for a description of LAPS), Rand's global sea surface temperatures from NCAR, 9-second DEM terrain height data from AUSLIG, and soil and vegetation classification data from CSIRO Wildlife and Ecology. The model was run with nested grids of 25 × 25 × 25 points at 30,000-m, 10,000-m, 3,000-m and 1,000-m spacing for meteorology, and 41 × 41 × 25 points at 15,000-m, 5,000-m, 1,500-m and 500-m spacing for pollution. Default model options were used, except with a deep soil moisture content that varied from 0.05 (very dry) for summer months to 0.25 (moist) for winter months. Tracer mode was used for sulfur dioxide, with the four dominant point sources (of the twenty point sources in the region) run in Lagrangian (LPM) mode. Land-use was dominated by grassland characteristics for most of the six sites in the monitoring network. More detail on the Kwinana region can be found in Hurley *et al.* (2001), which also presents TAPM V1.0 results.

Model predictions were extracted at the nearest grid point to each of the six monitoring sites on the inner grid (1,000-m grid spacing) at the lowest model level (10 m above the ground) for winds and temperature. Statistics of observations and model predictions are shown in Table 2.4. The statistics used were based on the recommendations of Willmott (1981), as described in the Appendix. The results suggest that both winds and temperature are predicted well.

The new results are marginally better than the already good results from TAPM V1.0 – see Hurley *et al.* (2001) for more detail on TAPM V1.0 results, although note that wind speed and the Naval Base site were not included in that paper. For winds at 10 m (averaged over wind speed and the wind components), the

- RMSE values for V1.0 and V2.0 are 2.3 and 2.4 m s^{-1} respectively;
- IOA values for V1.0 and V2.0 are 0.78 and 0.80 respectively.

For temperature at 10 m, the

- RMSE values for V1.0 and V2.0 are 2.4 and 2.3ºC respectively;
- IOA values for V1.0 and V2.0 are 0.95 and 0.96 respectively.

Table 2.4. Statistics for TAPM V2.0 simulation of 1997 in Kwinana (averaged over 6 sites) for wind speed at 10 m above the ground (WS10); the west-east-component of the wind (U10); the south-north-component of the wind (V10); and temperature (T10).

VARIABLE	NUMBER	MEAN_OBS	MEAN_MOD	STD_OBS	STD_MOD	CORR	RMSE	RMSE_S	RMSE_U	IOA	SKILL_E	SKILL_V	SKILL_R
WS10	7672	3.6	5.3	1.9	2.1	0.72	2.54	2.01	1.50	0.67	0.84	1.22	1.47
U10	7672	-0.1	-0.3	3.0	4.4	0.85	2.55	0.95	2.34	0.87	0.80	1.53	0.88
V10	7672	1.1	1.0	2.4	3.5	0.82	2.25	1.01	2.00	0.84	0.92	1.62	1.03
T10	8111	18.4	18.0	5.4	5.8	0.92	2.31	0.51	2.23	0.96	0.41	1.07	0.43

KEY: OBS = Observations, MOD = Model Predictions, NUMBER = Number of hourly-averaged values used for the statistics, MEAN = Arithmetic mean, STD = Standard Deviation, CORR = Pearson Correlation Coefficient (0 = no correlation, 1 = exact correlation), RMSE = Root Mean Square Error, RMSE_S = Systematic Root Mean Square Error, RMSE_U = Unsystematic Root Mean Square Error, IOA = Index of Agreement (0 = no agreement, 1 = perfect agreement), SKILL_E = (RMSE_U)/(STD_OBS) (<1 shows skill), SKILL_V = (STD_MOD)/(STD_OBS) (near to 1 shows skill), SKILL_R = (RMSE)/(STD_OBS) (<1 shows skill).

Note that both versions of TAPM tend to overestimate the wind speed (and hence standard deviations of the wind components) at several of the sites, but we suspect that this is due to near-site localised effects. The comparison between the model and the two most representative sites (Hope Valley and Naval Base) does not show any significant bias in wind speed, and has better statistics than the averages over all sites as a result.

Predicted sulfur dioxide concentrations at the monitoring sites are summarised for

- TAPM (V1.0 and V2.0).
- the Kwinana region regulatory model DISPMOD (Rayner, 1998, 2000), run in default regulatory mode. DISPMOD is the regulatory model for the Kwinana region, which has been developed and refined for the region over many years.
- and the EPA Victoria regulatory model AUSPLUME (Lorimer, 1986), run in default mode with Pasquill-Gifford dispersion curves used for source heights less than 100 m, and Briggs rural dispersion curves used for source heights greater than 100 m. This choice of dispersion curves was shown by Hamilton (1999) to give the best results for point source dispersion in Melbourne.

Note that from a theoretical viewpoint, AUSPLUME should not strictly be used for the Kwinana region (or, for that matter, in any coastal region), as the sources are within a few kilometres from the coast, and shoreline fumigation is the most important phenomenon affecting ground level concentrations. However, we have chosen to use it here due to its wide and varied use throughout Australia and New Zealand, and the fact that in practice it is commonly applied in coastal regions.

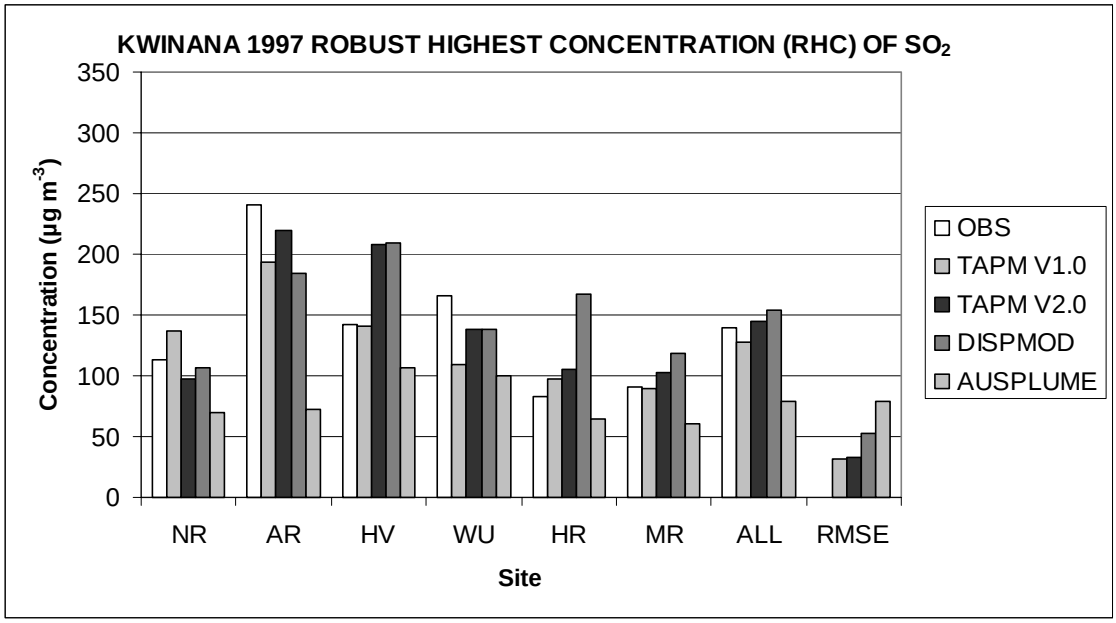

Figure 2.3. Kwinana 1997 predicted versus observed Robust Highest Concentration (RHC) at each of the monitoring sites, and for the average over all sites (ALL), for models TAPM V1.0 and V2.0, DISPMOD and AUSPLUME.

Figure 2.3 shows the Robust Highest Concentration (RHC) of sulfur dioxide for each model at each site and for the average over all sites. The RHC approach is from Cox and Tikvart (1990), using the mean of the top ten concentrations, and the 11th highest concentration, to

project to a robust measure of the highest concentration. The results show that TAPM V2.0 is performing well for all sites, and although there is more of an over-prediction at Hope Valley (HV) compared to V1.0, the under-prediction at Wattleup (WU) with TAPM V1.0 is not present in TAPM V2.0 results. This has made TAPM V2.0 slightly conservative and the best of all models shown. Overall, TAPM and DISPMOD are performing well, but AUSPLUME is under-predicting at the high end of the distribution. This can be illustrated by the ratio of RHC (predicted/observed for ALL), which for TAPM V1.0 is 0.92, for TAPM V2.0 is 1.04, for DISPMOD is 1.10, and for AUSPLUME is 0.57.

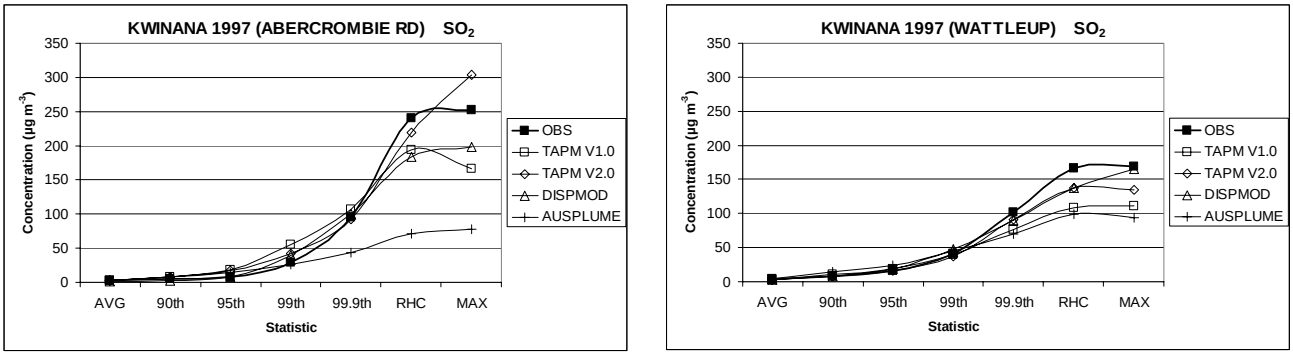

Figure 2.4. Observed and predicted statistics (Average (AVG), Percentiles (90^{th}, 95^{th}, 99^{th}, 99.9^{th}), Robust Highest Concentration (RHC) and Maximum (MAX)) of sulfur dioxide concentrations at Abercrombie Road (left) and Wattleup (right) monitoring sites in 1997.

Figure 2.4 shows statistical results from each model plotted against observations for Abercrombie Road (AR) and Wattleup (WU). The plots show average (AVG), 90^{th}, 95^{th}, 99^{th} and 99.9^{th} Percentiles, Robust Highest Concentration (RHC), and maximum concentration (MAX). These plots show that both TAPM and DISPMOD are doing a good job at all concentration levels, while AUSPLUME is under-predicting at all sites (especially at Abercrombie Road). These plots also illustrate the advantage of using percentiles or RHC, rather than the MAX concentration, to examine model performance or to get a more robust estimate of likely extreme concentrations at a site.

3 Annual urban meteorology and air pollution in Melbourne

Melbourne (144°53′E, 37°49′S) is a coastal city in the southern part of Victoria, Australia, with ocean to the south and mountains to the north. The EPA Victoria operates an air monitoring network covering the urban region of Melbourne, and measures both near-surface meteorology and air pollution (see Figure 3.1). This Section summarises the results from TAPM modelling of year-long (July 1997 to June 1998) meteorology and photochemical air pollution in Melbourne (Hurley *et al*., 2002), which was an update/extension of the verification component of the work performed as part of the EPA Victoria Air Quality Improvement Plan (Ng and Boyle, 2002).

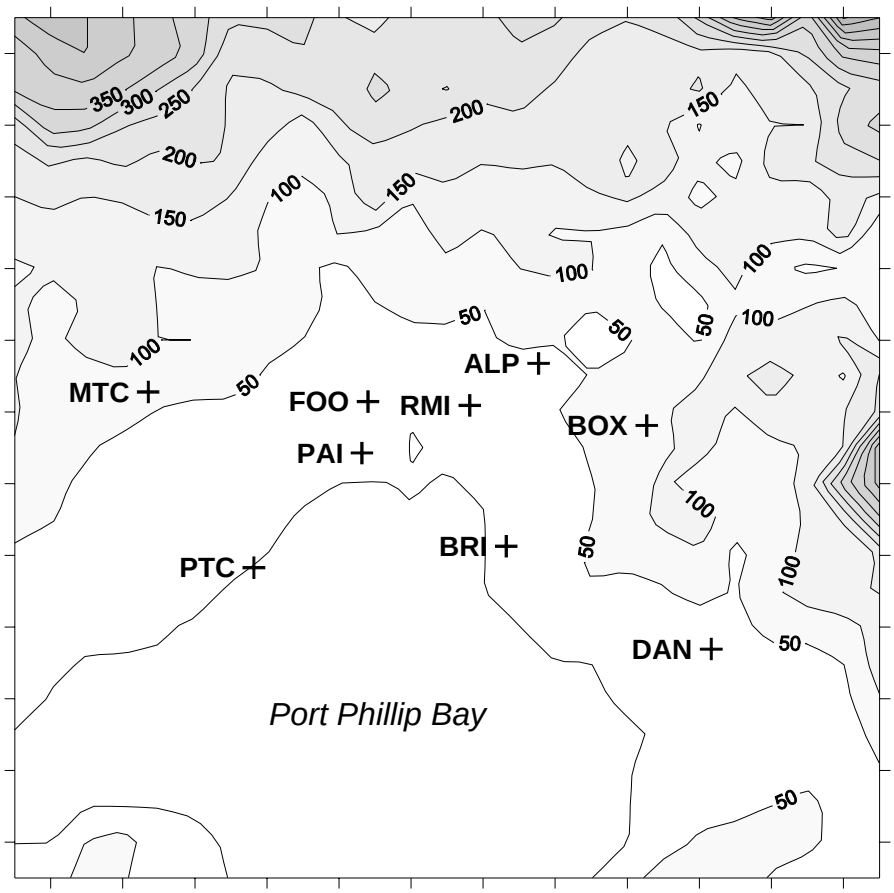

Figure 3.1. TAPM inner grid domain for Melbourne at 3000-m resolution with a west-east and south-north extent of 72 km. Terrain height (m) contours with shading for higher heights are shown. The EPAV monitoring sites are marked, and correspond to: Alphington (ALP), Box Hill (BOX), Brighton (BRI), Dandenong (DAN), Footscray (FOO), Mt. Cottrell (MTC), Paisley (PAI), Pt. Cook (PTC) and RMIT (RMI).

TAPM was configured with three (nested) grids of 25 × 25 × 25 points at 30,000-m, 10,000-m and 3,000-m spacing for meteorology, and 41 × 41 × 25 points at 15,000-m, 5,000-m and 1,500-m spacing for pollution. Default model options were used, except that deep soil moisture content varied from 0.05 (very dry) for summer months to 0.25 (moist) for winter months. Land-use was dominated by urban characteristics for most of the nine Melbourne monitoring sites. The simulations used as model input six hourly LAPS analyses at a grid spacing of 0.75° from the Bureau of Meteorology to provide the synoptic conditions (see Puri

et al., 1998, for a description of LAPS), Rand's global sea surface temperatures from NCAR, 9-second DEM terrain height data from AUSLIG, and soil and vegetation classification data from CSIRO Wildlife and Ecology.

The emissions inventory covered Melbourne and Geelong, as well as major point sources in the Latrobe Valley about 100 km east of Melbourne. It represents emissions for all pollutants on approximately a 1-km spaced grid for vehicle, commercial and domestic emissions, as well as a point-source inventory, and a biogenic-emission inventory on a 3-km spaced grid (nitrogen oxides and hydrocarbons only). The emission inventory was developed for the Melbourne region by EPA Victoria for both general EPA use, and for use by the Australian Air Quality Forecasting System (AAQFS) (Ng and Wong, 2002). Non-zero background concentrations were used for ozone (15 ppb), smog reactivity (Rsmog = 0.7 ppb) and particles (10 $\mu g\ m^{-3}$ for PM_{10} and 5 $\mu g\ m^{-3}$ for $PM_{2.5}$, to account for dust and sea salt emissions not in the inventory), and the standard reactivity coefficient for Rsmog of 0.0067 was used for all VOC emissions.

In order to examine the sensitivity of pollution results to predicted winds when simulating urban air pollution, the model was run twice. The first run (denoted by TAPM) was in normal mode without meteorological data assimilation, and the second run (denoted by TAPM#) was in data assimilation mode using Melbourne and Geelong monitoring site 10-m level wind speed and direction data. This second run used data assimilation site characteristics with a 20,000-m radius of influence, and assimilated the observed winds for the lowest three model levels (10 m, 25 m and 50 m).

Table 3.1. Statistics for TAPM V2.0 simulation without meteorological data assimilation of July 1996 – June 1997 in Melbourne (averaged over eight sites) for wind speed at 10 m above the ground (WS10); the west-east-component of the wind (U10); the south-north-component of the wind (V10); and screen-level temperature (TEMP).

VARIABLE	NUMBER	MEAN_OBS	MEAN_MOD	STD_OBS	STD_MOD	CORR	RMSE	RMSE_S	RMSE_U	IOA	SKILL_E	SKILL_V	SKILL_R
WS10	8295	3.3	3.5	1.9	1.8	0.73	1.43	0.68	1.28	0.85	0.70	1.00	0.78
U10	8295	0.8	1.1	2.1	2.2	0.75	1.57	0.55	1.47	0.86	0.72	1.08	0.78
V10	8295	0.3	0.1	3.0	3.1	0.85	1.69	0.47	1.63	0.92	0.55	1.03	0.58
TEMP	8621	14.6	14.8	5.9	6.4	0.92	2.37	0.75	2.24	0.95	0.38	1.07	0.40

KEY: OBS = Observations, MOD = Model Predictions, NUMBER = Number of hourly-averaged values used for the statistics, MEAN = Arithmetic mean, STD = Standard Deviation, CORR = Pearson Correlation Coefficient (0 = no correlation, 1 = exact correlation), RMSE = Root Mean Square Error, RMSE_S = Systematic Root Mean Square Error, RMSE_U = Unsystematic Root Mean Square Error, IOA = Index of Agreement (0 = no agreement, 1 = perfect agreement), SKILL_E = (RMSE_U)/(STD_OBS) (<1 shows skill), SKILL_V = (STD_MOD)/(STD_OBS) (near to 1 shows skill), SKILL_R = (RMSE)/(STD_OBS) (<1 shows skill).

Model predictions of meteorology (for the model run without meteorological data assimilation) were extracted at the nearest grid point to each of the eight meteorological monitoring sites on the inner grid (3,000-m spacing) at 10 m above the ground for winds and at screen-level for temperature. Statistics of observations and model predictions are shown in Table 3.1, and are based on the recommendations of Willmott (1981), including the Root

Mean Square Error (RMSE) and the Index of Agreement (IOA). The IOA is a measure of how well predicted variations about the observed mean are represented, with a value greater than about 0.50 considered to be good, as judged by several other published prognostic modelling studies (see Hurley, 2000). The results suggest that both winds and temperature are predicted very well, with no significant biases, low RMSE and high IOA. The average RMSE and IOA for winds are 1.6 m s^{-1} and 0.88, and for temperature are 2.4 C and 0.95, which are very good results.

Ground-level pollution results for hourly average NO_2 and O_3, and for daily average PM_{10} and $PM_{2.5}$, and Robust Highest Concentration (RHC) were extracted from the nearest grid point to each of the monitoring sites on the inner grid (1,500-m spacing), and are summarised in Figures 3.2 and 3.3 respectively. These results show that both TAPM and TAPM# simulations of the extreme concentrations are very good.

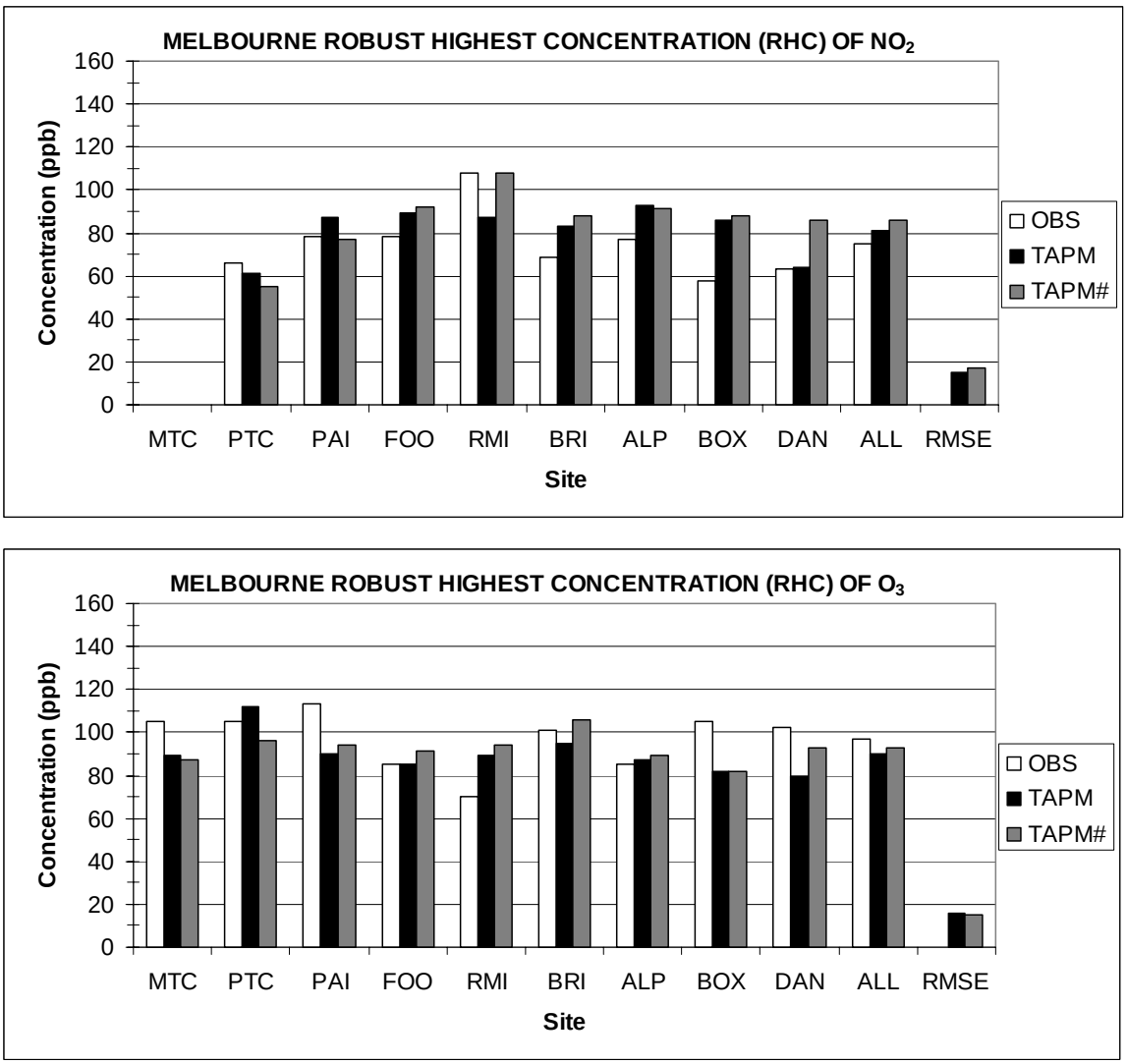

Figure 3.2. Nitrogen dioxide (top) and ozone (bottom) Robust Highest Concentration (RHC) values for each monitoring site and for the average over all sites, for TAPM (without wind data assimilation) and TAPM# (with wind data assimilation).

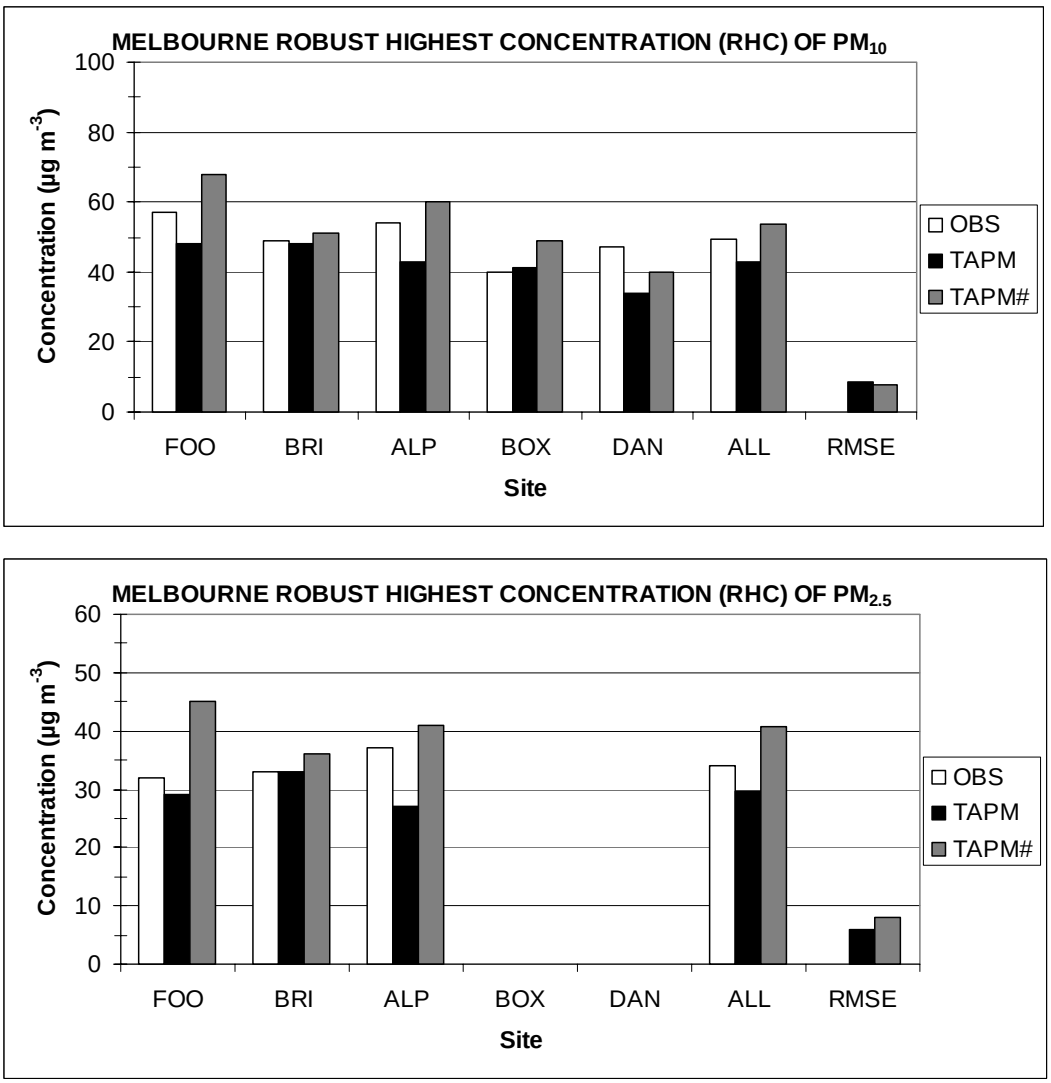

Figure 3.3. PM_{10} (top) and $PM_{2.5}$ (bottom) Robust Highest Concentration (RHC) values for each monitoring site and for the average over all sites, for TAPM (without wind data assimilation) and TAPM# (with wind data assimilation).

Figure 3.4 shows statistical results for NO_2 and O_3 for Footscray (FOO) and Brighton (BRI) monitoring sites, including average (AVG), 90^{th}, 95^{th}, 99^{th} and 99.9^{th} Percentiles, Robust Highest Concentration (RHC), and maximum concentration (MAX). These plots illustrate that TAPM is doing a good job at all concentration levels.

In summary, RHC ratios (predicted/observed, averaged over all sites) for

- nitrogen oxides (not shown in the Figures) are 0.88 for TAPM and 1.00 for TAPM#,
- nitrogen dioxide are 1.09 for TAPM and 1.15 for TAPM#,
- ozone are 0.93 for TAPM and 0.96 for TAPM#,
- PM_{10} are 0.87 for TAPM and 1.09 for TAPM#,
- and $PM_{2.5}$ are 0.87 for TAPM and 1.20 for TAPM#,

which indicates that there is very little bias in results (1.00 is perfect) at the extreme end of the concentration distribution for all pollutants. TAPM without data assimilation does as good a job as TAPM# with wind data assimilation for NO_2 and O_3, although for particles and

nitrogen oxides, TAPM# does slightly better overall – the extremes for these pollutants are controlled by low wind speed and low mixing, which occur overnight in winter.

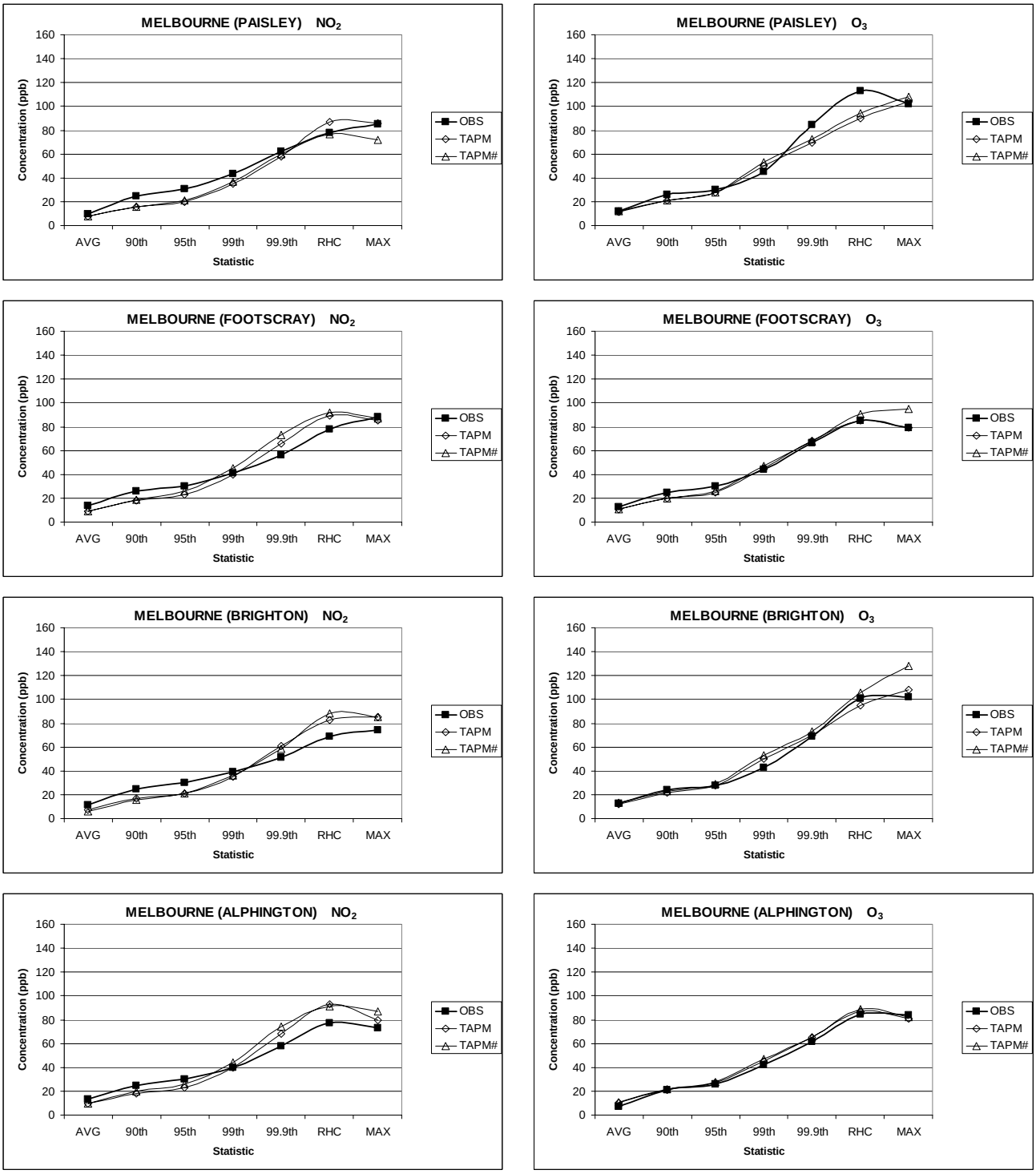

Figure 3.4. Nitrogen dioxide (left) and ozone (right) statistics at the Paisley, Footscray, Brighton and Alphington monitoring sites (Average (AVG), 90^{th} – 99.9^{th} Percentiles, Robust Highest Concentration (RHC) and Maximum (MAX)), for OBS (observed), TAPM (without wind data assimilation) and TAPM# (with wind data assimilation).

4 Annual urban meteorology and air pollution in Perth

Perth (32ºS, 116ºE), with a population of about 1.2 million people, is situated on a relatively straight north-south coastline in the south-west corner of Australia (Figure 4.1). The 300 m-high Darling Scarp rises sharply along the eastern edge of the coastal plain, about 25 km inland. Characteristic summer days consist of offshore easterly synoptic winds with strong south-westerly sea breezes in the afternoon, leading to a re-circulation of Perth's morning emissions back onshore. This Section presents results from a year-long TAPM simulation (1999) using motor vehicle, commercial/domestic, industrial and biogenic emissions inventories provided by the Department of Environmental Protection of Western Australia (DEPWA). TAPM results were compared to data from three DEPWA monitoring stations, chosen for their coastal (Swanbourne), outer-suburban (Caversham, 21 km inland) and rural (Rolling Green, 55 km inland) locations. These results are part of a study undertaken for Environment Australia to investigate the feasibility of using population-based emissions inventories in areas where emissions are not known (Physick and Cope, 2001; Physick *et al.*, 2002a).

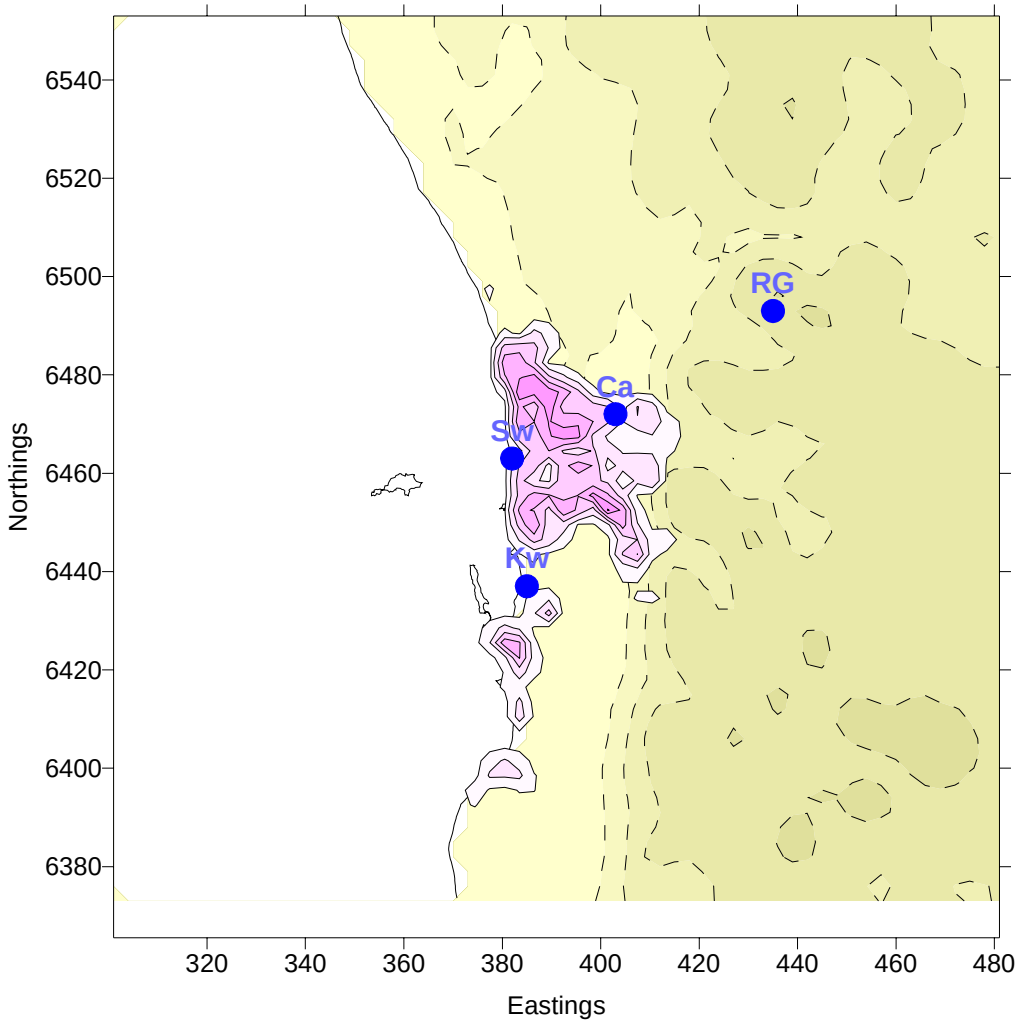

Figure 4.1. Map of the Perth region showing the monitoring sites Swanbourne (Sw), Caversham (Ca) and Rolling Green (RG), and the industrial complex site at Kwinana (Kw). Shaded areas indicate population density and dashed lines are heights above sea level from 50 m at an interval of 100 m.

4.1 Model configuration and emissions

Meteorological simulations were carried out on three nested grids (each 30 × 30 × 20 grid points) with grid spacings of 30, 10 and 3 km. The air quality simulations were done on the same grids, centred at (-31º59.5′, 115º45′) – approximately 10 km southwest of the Perth central business district. Terrain elevation was obtained from AUSLIG data (250 m resolution). The Swanbourne and Caversham sites were located within the 3-km spaced domain, but Rolling Green was on the coarser 10-km spacing domain. The motor vehicle, commercial/domestic and biogenic area inventories consist of emissions at 3-km intervals on a 40 × 40 grid centred at the same location as the model grid.

Vehicle emissions were specified with a diurnal profile for petrol exhaust, petrol evaporation and diesel exhaust. Files were also provided for a weekday, a Saturday and a Sunday. All emissions are for 25^{o}C, with a temperature correction being applied each timestep by the model. *Emissions from industry* were supplied as both surface area files and elevated point source files. The surface emissions vary hourly (but not daily), but there is no time variation in the point source files. TAPM uses source characteristics to calculate the plume-rise height for each point source. *Commercial/domestic emissions* varied diurnally, and also contained a weekday versus weekend variation. *Biogenic VOC emissions* were provided at 30^{o}C and a photosynthetic active radiation level (PAR) of 1000 μmol m^{-2} s^{-1}. When biogenic emissions are input in this way, the model is able to calculate hourly VOC emissions that are a function of temperature and PAR.

A background value of 20 ppb was assigned for ozone. The photochemistry equations in TAPM are formulated in terms of the smog-producing reactivity Rsmog, defined as VOC concentration multiplied by an activity coefficient for smog production. The value of the coefficient differs between VOC species, but an appropriate value for the VOC mix in an urban air mass is considered to be 0.0067 ppm/ppmC (Johnson *et al*., 1990). This value was used here to multiply emission rates for all VOC sources. It is also necessary to assign a background value for Rsmog, partly to account for a general background concentration of VOCs but also to compensate for the omission of some inorganic radical-producing reactions in the GRS photochemical mechanism. After some preliminary simulations, a value of 1.0 was chosen. Details of experiments examining the sensitivity of results to the background value of Rsmog can be found in Appendix A of Physick and Cope (2001).

4.2 Meteorological Results

Annual statistics for wind speed, east-west and north-south components of the wind, and temperature, all at a height of 10 m above the ground, have been extracted for the TAPM simulation and are presented in Table 4.1 as averages over the three sites. Statistics for the sites on the 3-km spaced grid (Swanbourne and Caversham) are especially good, as is the annual mean wind speed at Rolling Green (on the 10-km spaced grid). In summary, the averaged statistics in Table 4.1 suggest that the meteorology of the Perth region is being well-simulated by TAPM, with no significant biases, low RMSE and high IOA. The average RMSE and IOA for winds are 1.7 m s^{-1} and 0.86, and for temperature are 2.7ºC and 0.95, which are very good results.

Table 4.1. Statistics for TAPM V2.0 simulation of 1999 in Perth (averaged over three sites) for wind speed at 10 m above the ground (WS10); the west-east-component of the wind (U10); the south-north-component of the wind (V10); and temperature (TEMP).

VARIABLE	NUMBER	MEAN_OBS	MEAN_MOD	STD_OBS	STD_MOD	CORR	RMSE	RMSE_S	RMSE_U	IOA	SKILL_E	SKILL_V	SKILL_R
WS10	8516	3.7	3.8	1.8	1.7	0.69	1.60	1.01	1.22	0.78	0.68	0.93	0.88
U10	8516	-0.6	-0.9	3.2	3.3	0.86	1.89	0.84	1.67	0.91	0.54	1.04	0.60
V10	8516	0.5	0.2	2.4	2.3	0.82	1.45	0.60	1.29	0.90	0.56	0.99	0.62
TEMP	8643	18.2	18.4	5.9	6.7	0.92	2.65	0.39	2.62	0.95	0.44	1.12	0.45

KEY: OBS = Observations, MOD = Model Predictions, NUMBER = Number of hourly-averaged values used for the statistics, MEAN = Arithmetic mean, STD = Standard Deviation, CORR = Pearson Correlation Coefficient (0 = no correlation, 1 = exact correlation), RMSE = Root Mean Square Error, RMSE_S = Systematic Root Mean Square Error, RMSE_U = Unsystematic Root Mean Square Error, IOA = Index of Agreement (0 = no agreement, 1 = perfect agreement), SKILL_E = (RMSE_U)/(STD_OBS) (<1 shows skill), SKILL_V = (STD_MOD)/(STD_OBS) (near to 1 shows skill), SKILL_R = (RMSE)/(STD_OBS) (<1 shows skill).

4.3 Pollution Results

Modelled and observed annual statistics for nitrogen dioxide and ozone at Swanbourne, Caversham and Rolling Green are shown in Figure 4.2.

For nitrogen dioxide at Rolling Green, well away from any emission sources, model agreement with observations is good. However, for nitrogen dioxide at Swanbourne and Caversham, the higher concentration percentiles are over-predicted by TAPM. These primarily occur between 2000 and 2400 Local Time (in model and observations) and are due to industrial sources, as is evident from the much better agreement with observations when the model is run without these sources (see *MODEL (No ind.)* curve in Figures 4.2). Further work is currently being carried out to examine this discrepancy.

The model results for ozone at Swanbourne and Rolling Green are excellent when compared to the observations. While the higher ozone values at Caversham are underestimated by about 12 ppb, the model's performance overall for ozone is very good.

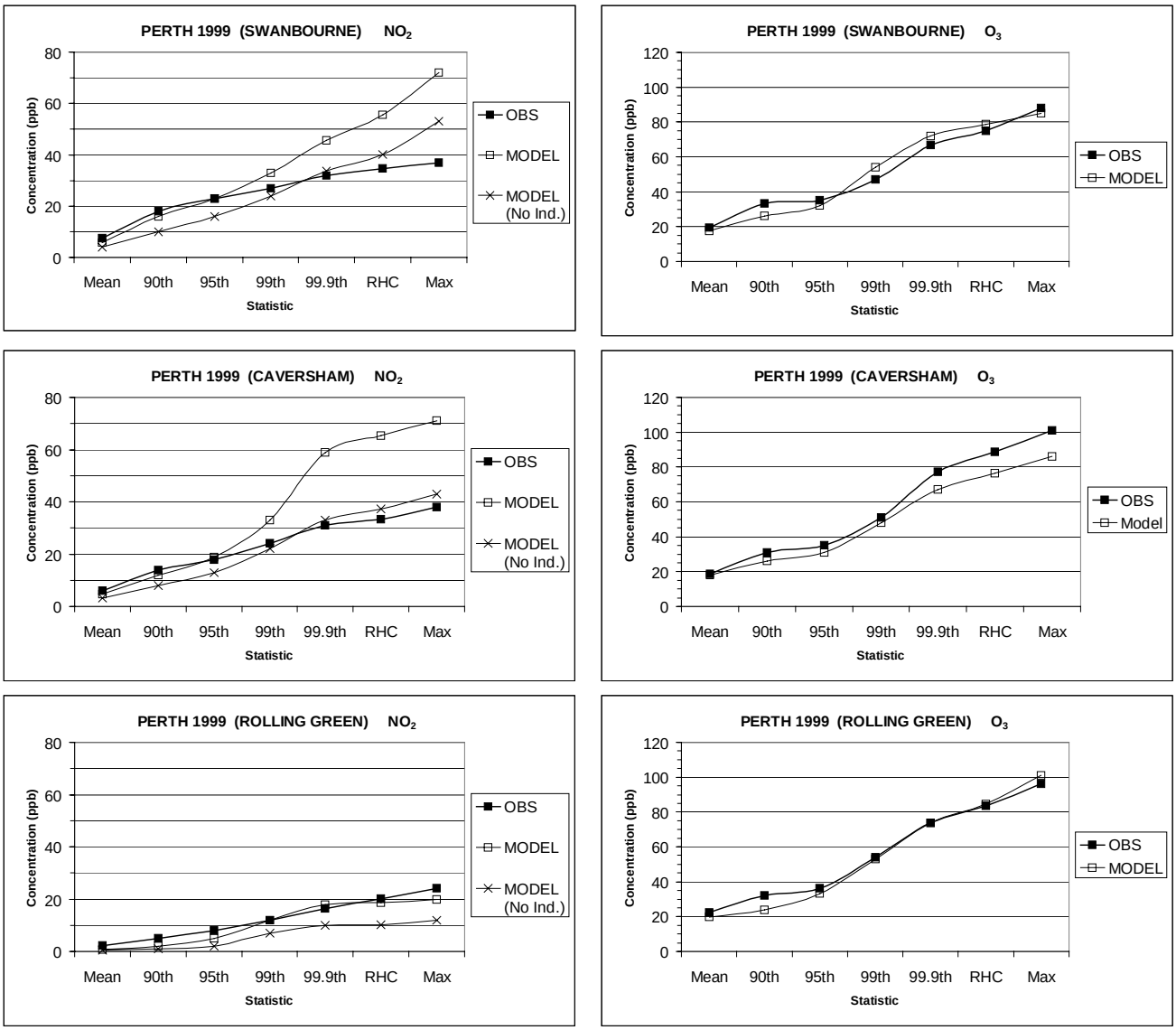

Figure 4.2. Nitrogen dioxide (left) and ozone (right) statistics at the Swanbourne (3-km grid), Caversham (3-km grid) and Rolling Green (10-km grid) monitoring sites (Average (Mean), 90^{th} – 99.9^{th} Percentiles, Robust Highest Concentration (RHC) and Maximum (Max)), for OBS (observed) and modelled (MODEL) concentration. Also shown are statistics for a simulation without industrial point sources (MODEL (no ind.)).

5 Meteorology and air pollution in the Pilbara

5.1 Surface meteorology and dispersion

The Pilbara region of Western Australia occupies a large part of the sparsely-populated north-west of the state. The coastal towns of Dampier and Karratha, 1500 km north of Perth, service local industry (established on the Burrup Peninsula as a result of offshore natural gas) and the ore-loading facilities set up to ship ore transported by rail from inland mining areas. Figure 5.1 shows a map of the area with monitoring sites and significant emitters of pollutants. To enable a greater understanding of the fate of emissions in this region, where the meteorology at scales important for dispersion is virtually unknown, the WA Department of Environmental Protection (DEPWA) initiated a Study to collect and analyse meteorological and air quality data in the region (Physick, 2001; Physick *et al*., 2000). It was established that low-level coastal winds in the Burrup Peninsula region were predominantly north-easterly to south-easterly from April to August, and north-westerly to south-westerly from September to March. However in those transition months between summer and winter, there were many days when the wind direction in the lowest 800 m backed through 360^o over a 24-hour period, often for several consecutive days. It was surmised that the wind behaviour on such days may lead to recirculation of coastal emissions back to the source region, and this was supported by some preliminary TAPM simulations. With the exception of PM_{10}, air quality levels near the sources in the Pilbara were found to be comfortably below National Environment Protection Measure (NEPM) standards, and are probably so throughout the region.

A following study (Physick and Blockley, 2001; Physick *et al*. 2002b) evaluated the suitability of three models, TAPM, DISPMOD and AUSPLUME, for application to the dispersion of emissions in the region. In this section, meteorological results from TAPM and ground-level concentrations from year-long simulations (1999) with all three models are compared with NO_x observations at the DEPWA monitoring station at Dampier and the Woodside station at King Bay (Figure 5.1). TAPM predictions of O_3 and NO_2 are also compared to data from the Dampier station.

5.1.1 Model configuration and emissions

TAPM V2.0 meteorological simulations were carried out on three nested grids (each 21 × 21 × 20 gridpoints) with grid spacings of 10, 3 and 1 km. The air quality simulations were done at twice the resolution (5, 1.5 and 0.5 km) on the same dimension grids, all centred at (–20^{o}39′S, 116^{o}43′E) to the southwest of Dampier. Terrain elevation was obtained from AUSLIG data (250 m resolution). For the 1-km grid, land-use classification in the data set accompanying the TAPM modelling package was changed from a land category to water for gridpoints corresponding to the Dampier Salt Farm at the lower end of the Burrup Peninsula. Emissions inventories in the form of surface area files and elevated point source files were provided by the Department of Environmental Protection of Western Australia (DEPWA). The DEPWA area emissions file (including biogenics) consisted of values at 1-km intervals on a 31 × 33 grid centred about 5 km east of Dampier.

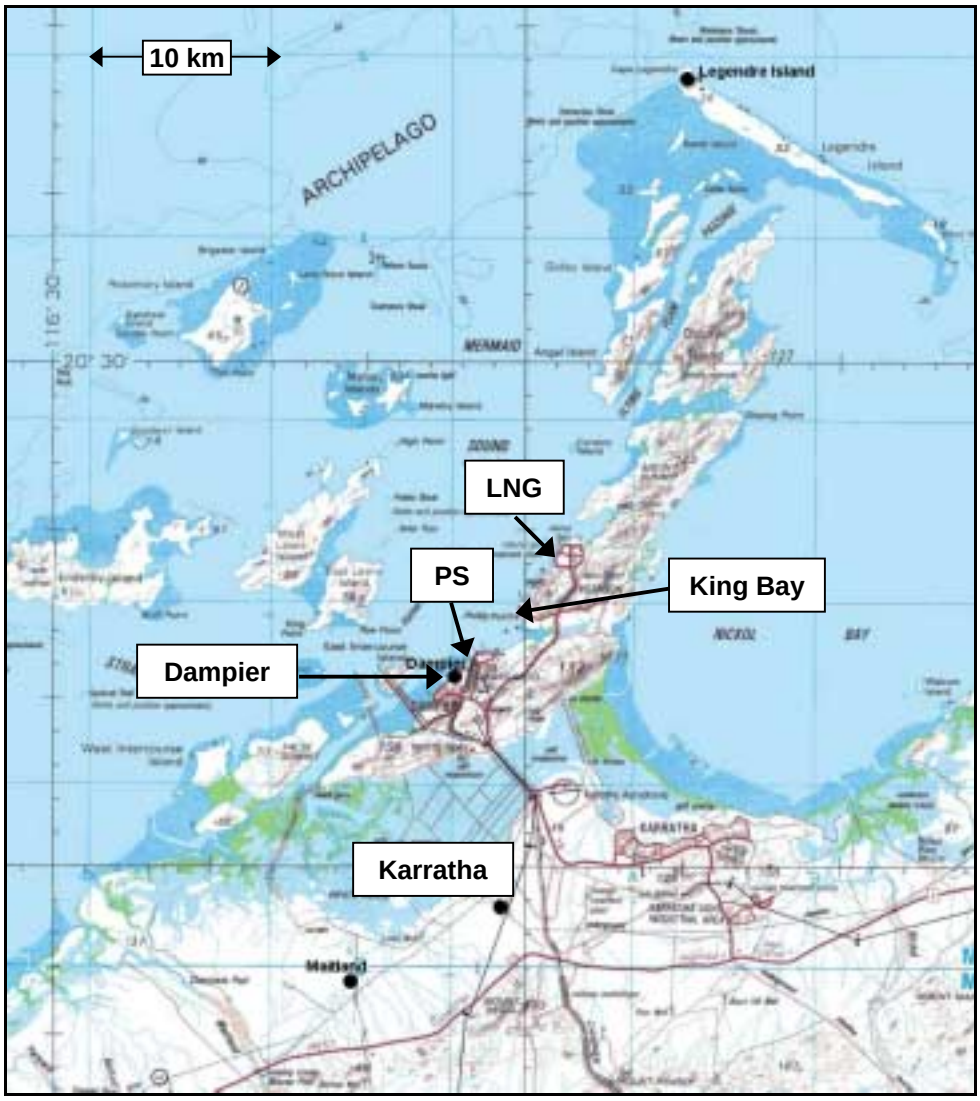

Figure 5.1. The Burrup Peninsula region, including the data sites, King Bay, Dampier and Karratha, and the emission point sources Dampier power station (PS) and the liquefied natural gas (LNG) plant.

There are currently two point-source complexes on the Burrup Peninsula. A total of 32 point sources were specified for the *Woodside liquefied natural gas plant (LNG)* site, with NO_x and VOCs being the dominant emissions. Knowing the individual emissions and reactivities of the main VOC constituents (parafin, toluene, xylene and benzene), a weighted activity coefficient of 0.0012 was calculated and used to obtain the emission rate of R_{smog} (activity coefficient multiplied by VOC emission rate) for input to TAPM. Emissions were not specified to vary hourly or daily, but quarterly. *Dampier power station* emissions for 1999 were specified for each hour for every day of the year. A buoyancy enhancement factor of 1.27 was calculated to take account of the 70-m spacing of the two stacks.

Area sources included Dampier and Karratha townships, several main roads, ship-loading facilities, the two main shipping lanes, and storage depots. Emissions from these sources remained constant for all hours of the year, and were small compared to LNG emissions. *Biogenic emissions* varied with time of day, but not with day of the year, so that vegetation

was assumed to emit at the same rate on both hot days and cool days. A background value of 25 ppb was specified for ozone for all months.

A factor to be taken into consideration when comparing model and data is that pollutant levels are enhanced in smoky air transported to the Burrup Peninsula from fire areas inland. Eighteen such days, identified by high PM10 levels and Bureau of Meteorology visibility reports from Port Hedland, were discarded from the NO_x and O_3 model comparisons. Analysis of the Dampier monitoring data suggests that peak O_3 values are increased by up to 20 ppb in smoky air. Further discussion can be found in Physick and Blockley (2001).

5.1.2 Meteorological results

Annual statistics for wind speed, east-west and north-south components of the wind, temperature and relative humidity, all at a height of 10 m above the ground, have been extracted for the TAPM simulation on the 1-km spaced grid and are presented in Table 5.1 for the Dampier and Karratha sites. At both sites, statistics are very encouraging as RMSEs are well below the standard deviation in the observations, the indexes of agreement are especially high, and at Dampier the variance in observations and model are very similar. The modelled temperature at Karratha shows more variability than is observed, mainly due to cooler temperatures at night on many occasions.

Table 5.1. Annual statistics at Dampier and Karratha for TAPM V2.0 simulation of 1999 for the following surface variables (10 m above the ground): wind speed (WS10), the west-east component of the wind (U10), the south-north component of the wind (V10), temperature (TEMP), and relative humidity (REL. H).

VARIABLE	NUMBER	MEAN_OBS	MEAN_MOD	STD_OBS	STD_MOD	CORR	RMSE	RMSE_S	RMSE_U	IOA	SKILL_E	SKILL_V	SKILL_R
DAMPIER													
WS10	8405	3.8	4.0	1.7	1.6	0.47	1.72	1.04	1.37	0.68	0.79	0.89	0.99
U10	8405	0.3	-0.3	3.3	3.5	0.83	2.09	0.76	1.95	0.90	0.59	1.04	0.63
V10	8405	0.0	0.2	2.5	2.5	0.74	1.87	0.71	1.72	0.85	0.68	1.00	0.74
TEMP	8668	25.8	25.6	3.9	4.3	0.90	1.88	0.14	1.88	0.94	0.49	1.12	0.49
REL. H	8633	60.9	60.6	18.2	18.1	0.74	12.99	4.73	12.10	0.86	0.67	1.00	0.71
KARRATHA													
WS10	8737	4.4	4.4	2.3	1.8	0.65	1.78	1.18	1.34	0.79	0.58	0.76	0.77
U10	8737	0.2	-0.4	4.1	3.6	0.86	2.17	1.19	1.81	0.92	0.44	0.86	0.53
V10	8737	-0.3	0.2	2.8	3.1	0.77	2.11	0.65	2.01	0.86	0.71	1.10	0.74
TEMP	8737	25.6	25.2	5.0	7.5	0.88	3.89	1.68	3.50	0.90	0.70	1.50	0.78
REL. H	8736	60.3	56.6	21.9	25.1	0.78	16.46	4.43	15.85	0.87	0.72	1.14	0.75

KEY: OBS = Observations, MOD = Model Predictions, NUMBER = Number of hourly-averaged values used for the statistics, MEAN = Arithmetic mean, STD = Standard Deviation, CORR = Pearson Correlation Coefficient (0 = no correlation, 1 = exact correlation), RMSE = Root Mean Square Error, RMSE_S = Systematic Root Mean Square Error, RMSE_U = Unsystematic Root Mean Square Error, IOA = Index of Agreement (0 = no agreement, 1 = perfect agreement), SKILL_E = (RMSE_U)/(STD_OBS) (<1 shows skill), SKILL_V = (STD_MOD)/(STD_OBS) (near to 1 shows skill), SKILL_R = (RMSE)/(STD_OBS) (<1 shows skill).

5.1.3 Results for NO_X

The Dampier monitoring station is on the coast, 9 km from the LNG plant and 1 km from the Dampier power station. The NO_x statistics for Dampier from the TAPM simulation on the 0.5-km spaced grid are shown in Figure 5.2. The model underestimates the RHC and 99.9th percentile concentrations by 30%, although the difference for the highest concentration for the year is only about 15%. Also shown in Figure 5.2 are statistics from DISPMOD and AUSPLUME simulations, using either an observed meteorology file from Dampier or a file consisting of TAPM-predicted meteorology at the LNG grid point. DISPMOD also used TAPM predicted stability profiles during onshore flow.

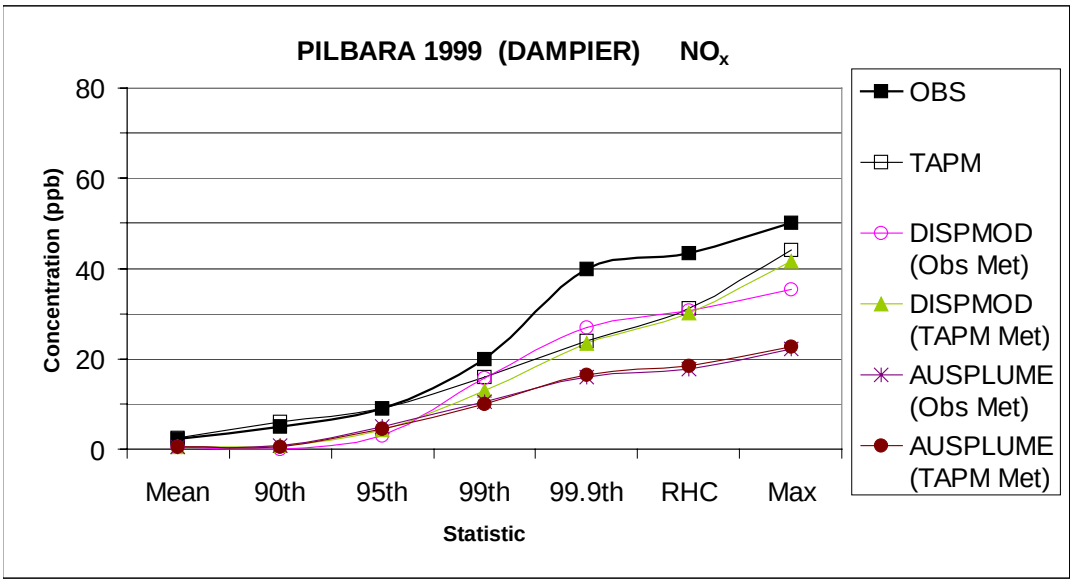

Figure 5.2. Annual mean, maximum, robust highest concentration (RHC) and percentile statistics for modelled (0.5-km grid) and observed nitrogen oxides at Dampier for 1999. The curves represent different models with alternative input, as detailed in the text.

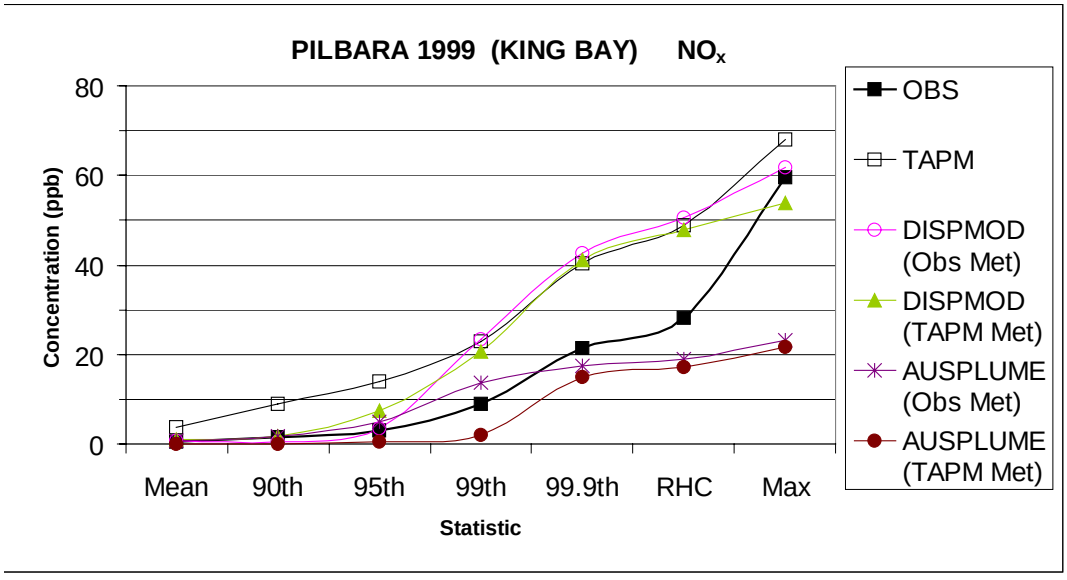

Figure 5.3. Same as for Figure 5.2, but at King Bay for 1999.

DISPMOD results, for both observed and predicted meteorology input, are very similar to the TAPM results, while the AUSPLUME concentrations are less than 50% of the observed values for all statistics. Note though that the input files for DISPMOD and AUSPLUME did not include area emissions. TAPM simulations with and without area sources indicate a difference of 5 ppb for the annual maximum glc and 4 ppb at the 99th percentile level.

The King Bay monitoring station is 4 km along the coast from the LNG plant. The statistics in Figure 5.3 show that TAPM and DISPMOD over-predict the RHC by about 60%, and the various percentiles by lesser amounts. The maximum concentration is estimated well by both models. AUSPLUME does best of the three models at King Bay for RHC and the percentiles, but does not predict the maximum of 60 ppb. Further discussion can be found in Physick *et al*. (2002b).

In summary, TAPM and DISPMOD perform satisfactorily in the Burrup Peninsula region, but an underestimate of concentrations at Dampier and an over-estimate at King Bay suggest that the modelled LNG plumes are being brought to the ground too close to the plant. The variability in atmospheric stability as the plumes travel along the irregular coastline from source to monitors is an especially difficult aspect for the models to simulate. AUSPLUME under-predicts the higher NO_x glcs at Dampier (by 50%) and this may be due to its inability to model the fumigation of elevated plumes.

5.1.4 Results for NO_2 and O_3

For the secondary pollutants NO_2 and O_3, model results are compared with data at the Dampier station. The modelled NO_2 results (from the 0.5-km spaced grid) in Figure 5.4 are in good agreement with the observations, although the maximum concentration is about 40% higher than observed. This case, in which the peak concentration is considerably higher than other concentrations, illustrates the value of the robust highest concentration (RHC), a statistic that mitigates the undesirable influence of unusual events.

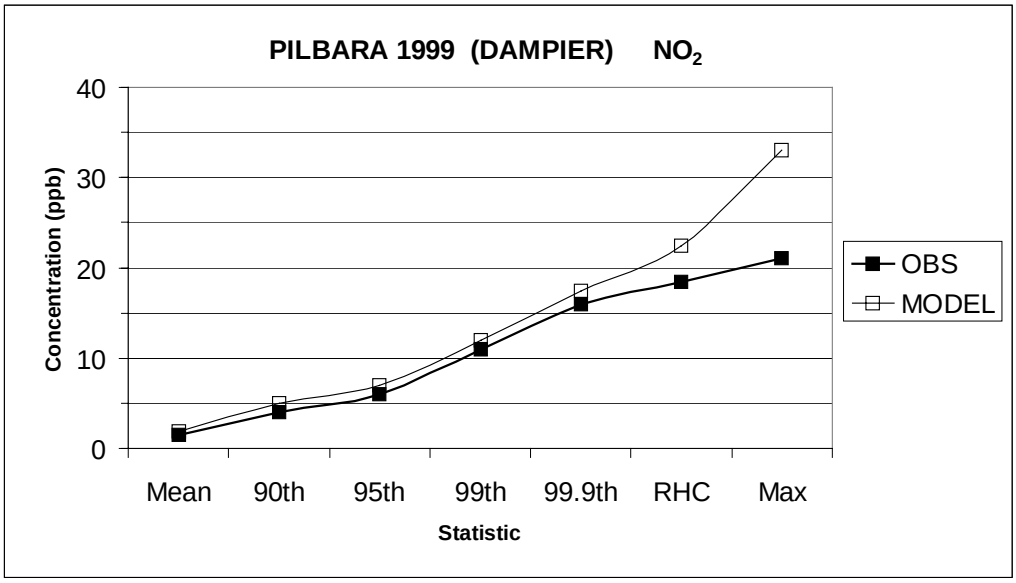

Figure 5.4. Annual mean, maximum, robust highest concentration (RHC) and percentile statistics for modelled (0.5-km grid) and observed nitrogen dioxide at Dampier for 1999.

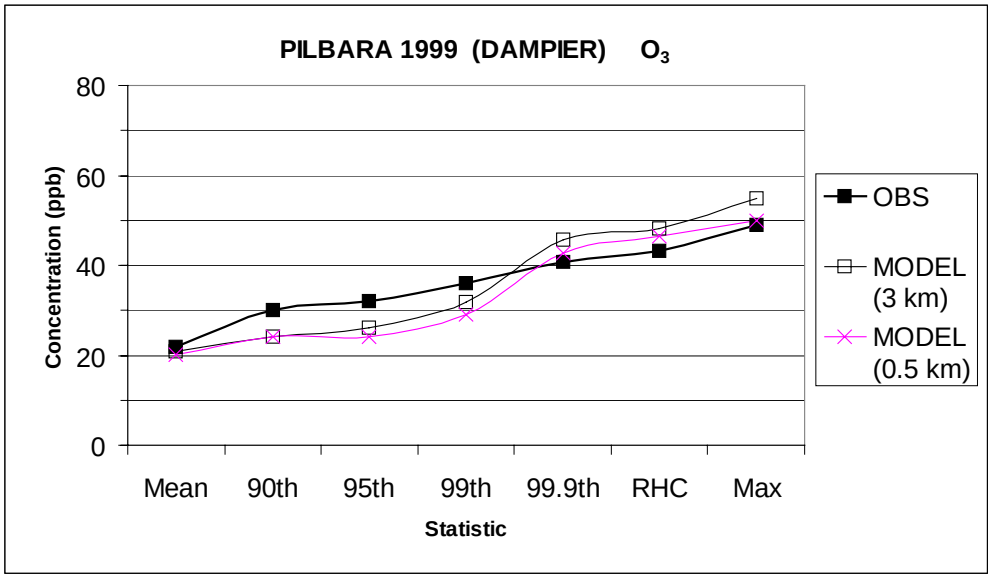

Figure 5.5. Annual mean, maximum, robust highest concentration (RHC) and percentile statistics for modelled (3-km grid) and observed ozone at Dampier for 1999.

Simulations for O_3 with various grid spacings showed that it is not necessary to use smaller spacings than 3 km, for either comparison with Dampier observations or when predicting a regional maximum. Figure 5.5 shows the modelled and observed annual statistics for O_3, for the 3-km and 0.5-km spaced grids, and it can be seen that the higher concentrations are simulated well. The middle-range of concentrations between 25 and 35 ppb is underestimated by the model, and this is reflected in the model's variance, which is only half that of the observations. Time series show that the diurnal amplitude of the ozone signal is often underestimated, including many occasions when the winds are steady from the south or east, suggesting that biogenic VOC emissions may not be large enough. However, this characteristic may also arise from assumptions in the GRS photochemical mechanism in TAPM, which lead to an under-production of radicals (M. Cope, personal communication, 2001).

5.2 Upper-air meteorology

5.2.1 Karratha

For the Burrup Peninsula region, TAPM simulations have been done for winter (July 1998) and summer (January 1999) months, as well as the seasonal transition months (April 1998 and October 1998). The model results were compared to observed surface and upper-air winds (half-hourly averaged acoustic radar data) at DEPWA's Karratha site. Monthly-mean winds were used in the analysis as a means of evaluating the model's ability to simulate the variation of the wind patterns with height and season.

Simulations were carried out on three nests centred on Karratha (each 40 × 40 × 20 gridpoints) with grid spacings of 30, 10 and 3 km. Vertical grid levels were at heights above the ground of 10, 50, 100, 150, 200, 300, 400, 500, 750, 1000, 1250, 1500, 2000, 2500, 3000, 4000, 5000, 6000, 7000 and 8000 m. Deep soil moisture content must be specified for each month, and test simulations showed that best results were obtained with 0.05 for January, April and October, and with 0.15 for July.

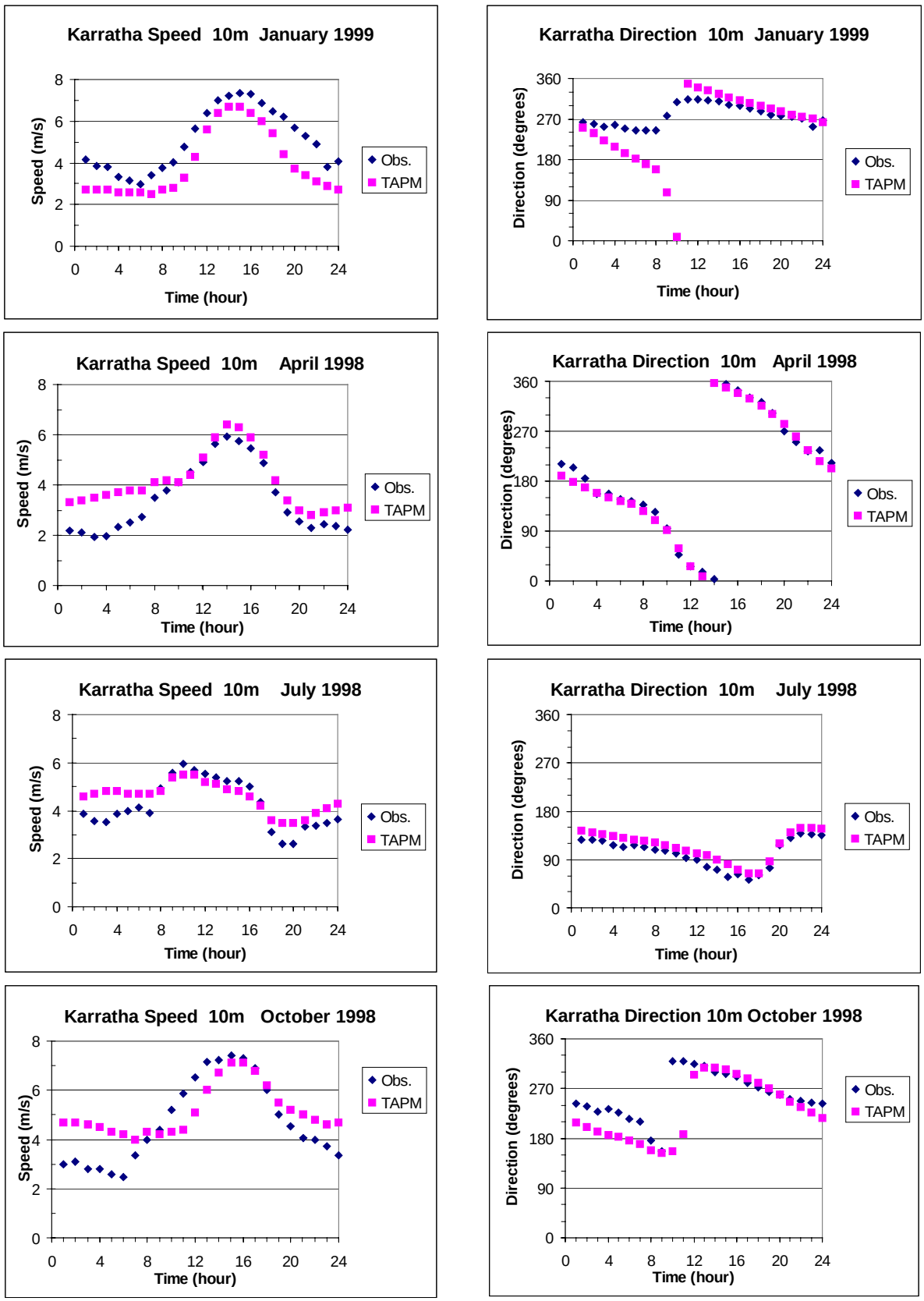

Figure 5.6. Diurnal variation of observed (◆) and modelled (■) monthly-mean wind speed and direction at a height of 10 m at Karratha for January 1999, April 1998, July 1998 and October 1998.

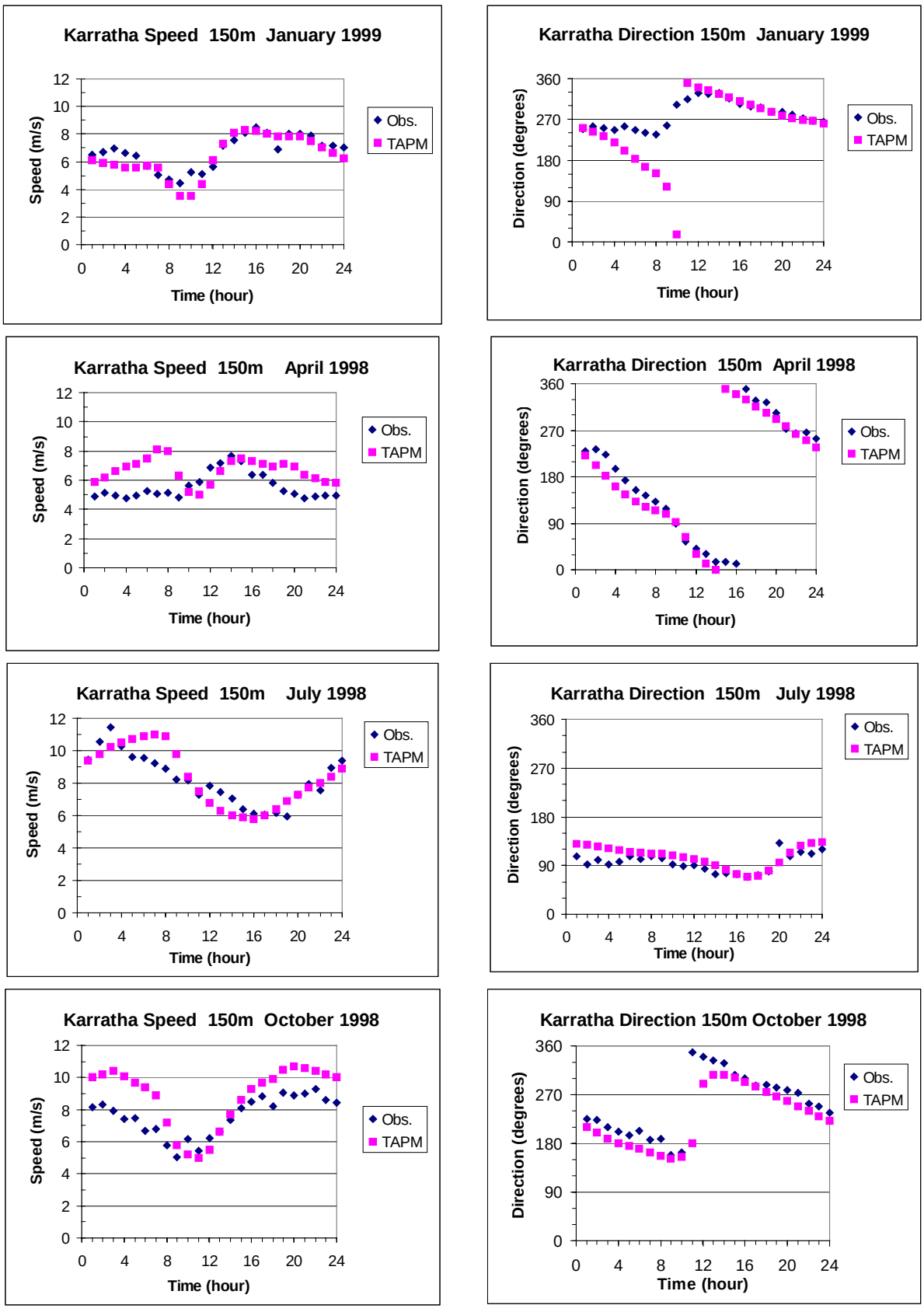

Figure 5.7. Diurnal variation of observed (◆) and modelled (■) monthly-mean wind speed and direction at a height of 150 m at Karratha for January 1999, April 1998, July 1998 and October 1998.

For the four months, Figure 5.6 shows the modelled and observed monthly-mean winds at a height of 10 m for each hour of the day. The highest speeds are observed in January and October, in mid-afternoon when the wind is off the sea, whereas the smaller maximum in July occurs at 0900 Local Time, probably arising from convective mixing of the nocturnal jet to the surface. TAPM reproduces the magnitude and timing of all these speed characteristics well. Wind direction is also simulated well, apart from a backing (as opposed to the observed veering) of the morning wind in January as it moves from offshore to onshore. Daily observations show that the wind can turn through either direction.

Figure 5.7 shows the mean winds at a height of 150 m above the ground. The diurnal speed patterns for each month at this height are quite different to those at 10 m, with a nocturnal jet most apparent in July. Modelled speed and direction are in good agreement with the observations, although a predicted speed maximum at 0700 Local Time in April is not observed. At both heights, the model tends to over-predict wind speed at night when the wind direction is between south-southwest and south-southeast. This appears to be related to a general drainage flow from sloping ground to the south, rising to the Hamersley Range, about 150 km south of Karratha.

5.2.2 Port Hedland

Monthly TAPM simulations have also been done for the Port Hedland region, 200 km east of Karratha. Port Hedland (20º18′S, 118º35′E) is primarily a shipping port for ore from mines in the inland Hamersley Range. At this location, the coastline runs approximately east-west, with the sea to the north. The model results were compared to observed upper-air winds from the twice-daily radiosonde flights at 0700 and 1900 Local Time at the Bureau of Meteorology's (BoM) station, 7 km from the coastline. The same months were simulated as for Karratha, except that April 1999 was substituted for April 1998 as the finer vertical-resolution radiosonde flights did not commence until July 1998. Monthly-mean winds up to a height of 1000 m were used in the comparison. Results were also compared to winds from BoM's LAPS model, run at the coarser grid spacing of 75 km. TAPM is nested within LAPS and thus obtains synoptic meteorological information from this model.

Simulations for the Port Hedland region were carried out on three nests centred on the BoM station. Each nest consisted of 41 × 41 × 20 gridpoints with grid spacings of 30, 10 and 3 km. Vertical grid levels were at the same heights above the ground as those for the Karratha simulation. Deep soil moisture content was specified as 0.05 for January and October, and 0.15 for April and July.

Figure 5.8 shows the profile comparisons for the four months at 0700 Local Time. Agreement with observations is good at all times of the year. For April and July, it is evident that the finer-scale model TAPM is able to capture the low-level jet at about 300 m, whereas the coarse vertical resolution in LAPS produces a weaker and more elevated jet. In October though, TAPM and LAPS predict jets that do not appear in the mean observations. Both models agree well with observed wind direction profiles, except in January when the mean LAPS direction is too southerly.

The predicted and observed wind profiles at 1900 Local Time are shown in Figure 5.9. The January speeds have increased from 0700 Local Time, due to a daytime sea-breeze effect. It is likely that the coarse horizontal resolution of LAPS limits its ability to produce sea breezes of the observed strengths. The low-level wind maxima observed in January and October have been reproduced, as have the well-mixed profiles in April and July, although wind speeds in

the latter months are under-predicted by 1–2 m s^{-1} above 200 m. In April, wind direction is too easterly by about 40 degrees, but agreement is very good for the other three months.

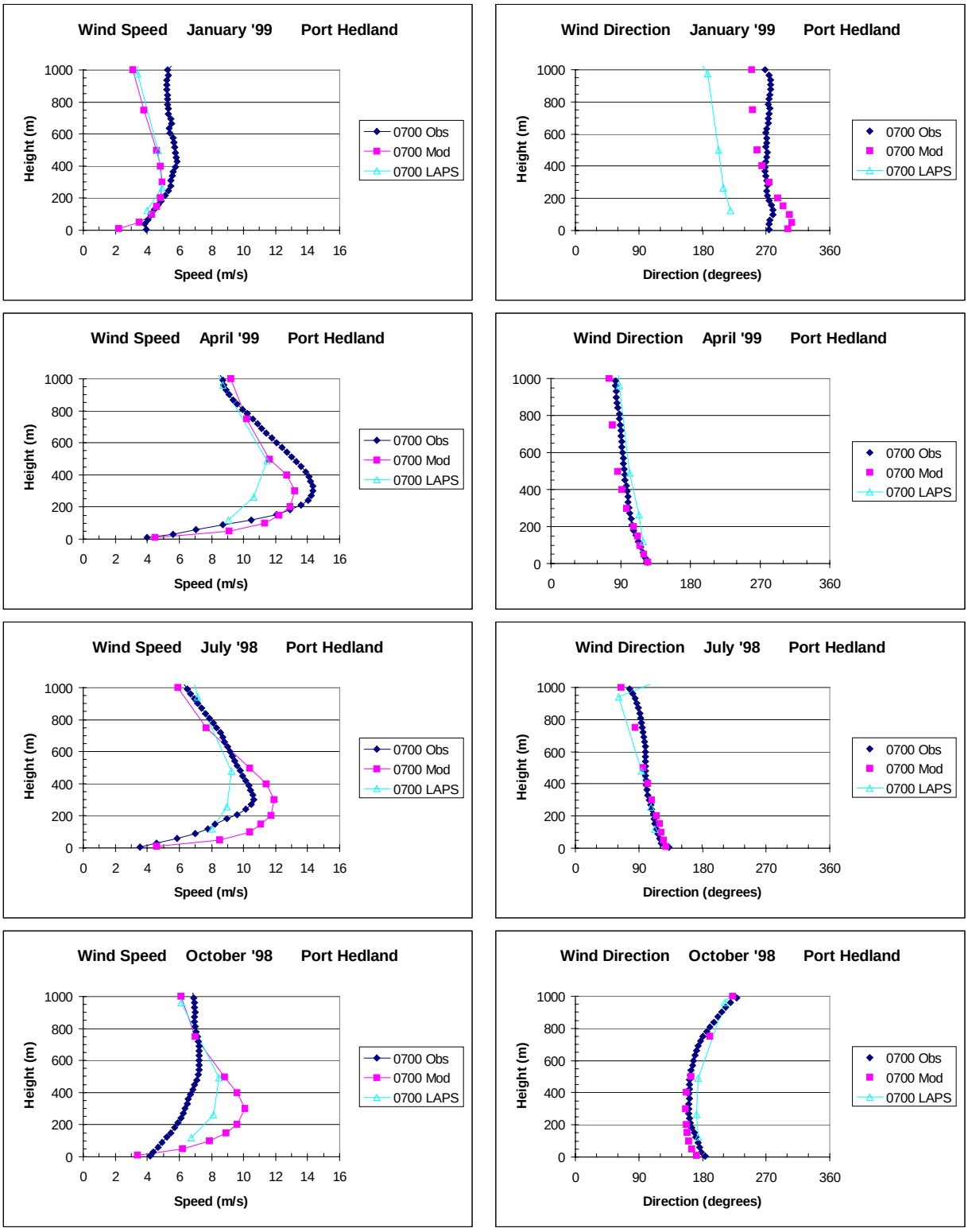

Figure 5.8. Diurnal variation of observed (◆) and TAPM modelled (■) monthly-mean wind speed and direction profiles at 0700 Local Time at Port Hedland for January 1999, April 1999, July 1998 and October 1998. Modelled LAPS profiles (Δ) are also shown.

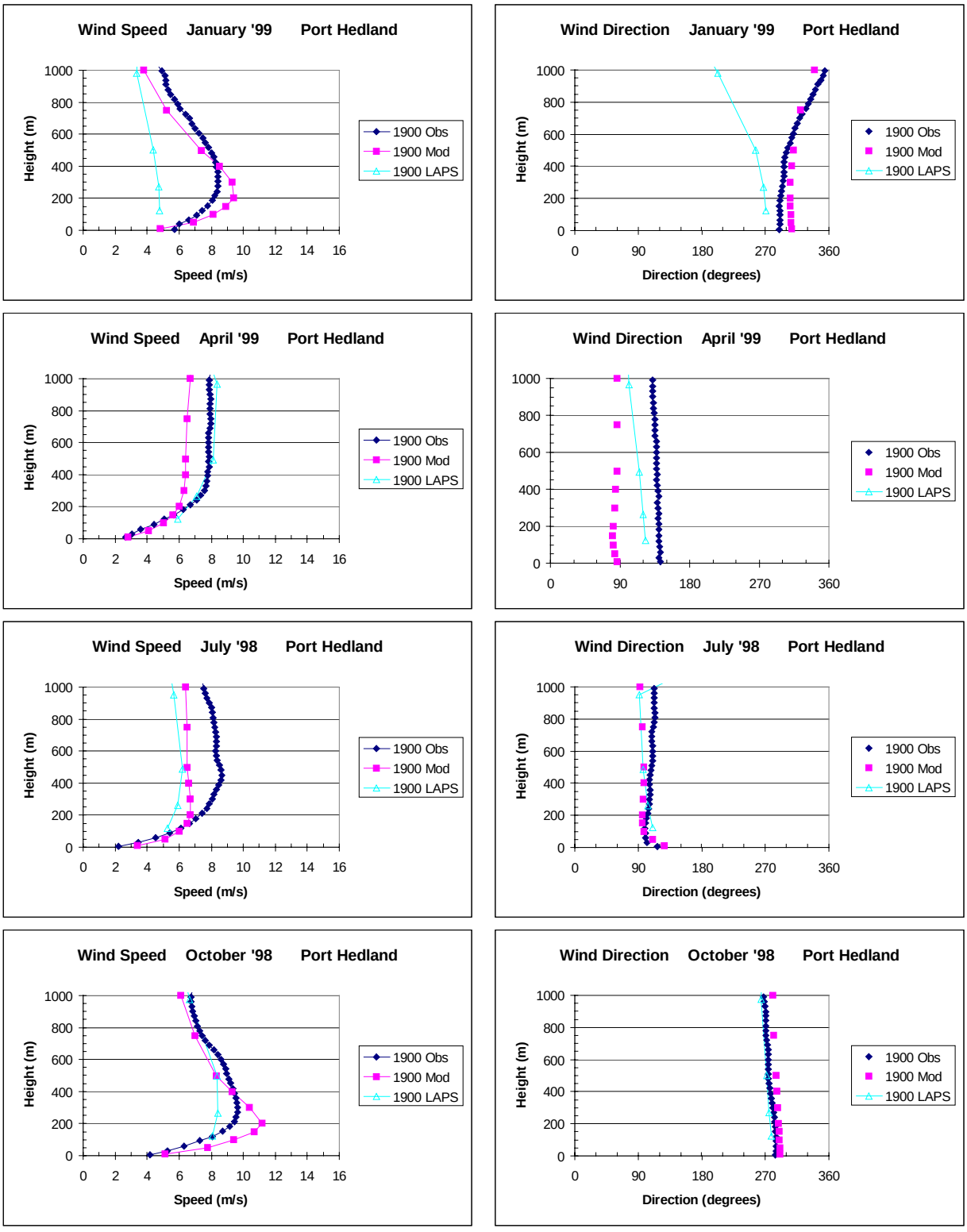

Figure 5.9. Diurnal variation of observed (◆) and TAPM modelled (■) monthly-mean wind speed and direction profiles at 1900 Local Time at Port Hedland for January 1999, April 1999, July 1998 and October 1998. Modelled LAPS profiles (Δ) are also shown.

5.2.3 Stability profiles at Port Hedland

A six-day period of field observations was carried out at Port Hedland from 28 March to 2 April 2000. Throughout each day, radiosondes measuring winds and temperatures were released simultaneously at the coastline and at the Bureau of Meteorology station 7 km inland. The objective of this work was to determine the thermal stability profile in the sea breezes that develop under the dominant east-southeasterly synoptic winds at this time of the year.

Surface winds and screen temperature at the coastal site (Figure 5.10) show a regular pattern of offshore south-easterly winds between midnight and about 0800 Local Time, and then a sea-breeze induced backing of the wind through east, north and west, reaching south again by midnight. TAPM results are also shown in Figure 5.10. There is good agreement with the observations for wind direction and screen temperature, while the model overestimates morning wind speed on some days.

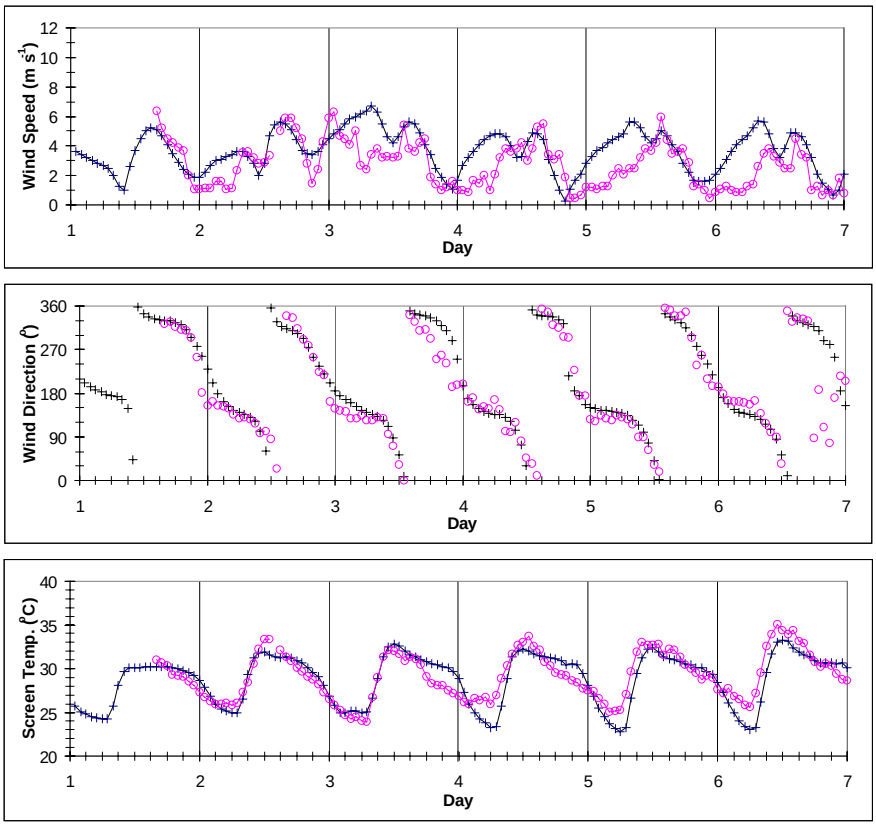

Figure 5.10. Observed (o) and TAPM modelled (+) wind speed and direction, and screen temperature observed at the Port Hedland coastal site, 28 March to 2 April 2000.

The most interesting finding from the coastal radiosonde flights was the different structure of the temperature profiles in the sea breeze on different days. Examples at the coastal site are shown for 28 March and 1 April in Figure 5.11 at 1600 Local Time, along with TAPM predictions. On both days, the mid-morning sonde flight sampled air flowing from the land, with typical mixed-layer profiles to heights of 400 m. However, on 28 March the mixed-layer air was cooler than the sea-surface potential temperature, so that the mixed layer was maintained as the air flowed over the sea. This process continued until the sea breeze set in at about 1100 Local Time. The air flowing onshore in the sea breeze for the rest of the day is

originally land air that crossed the coast further to the east earlier in the morning. Consequently, this onshore flow should be well-mixed. The flow at this time is from the north, normal to the coastline, and the depth of the mixed layer (250 m) is determined by the depth of the inflow. The important difference between the two days for plume dispersion is the stability profile between the heights of 50 m and 300 m. Buoyant coastal plumes with heights in this range would be mixed to the surface on 28 March, whereas on 1 April they would be carried inland aloft and fumigated to the ground further inland. The profiles predicted by TAPM show good agreement with the observations, for the temperature values and, more importantly, for the variation with height of the thermal stability.

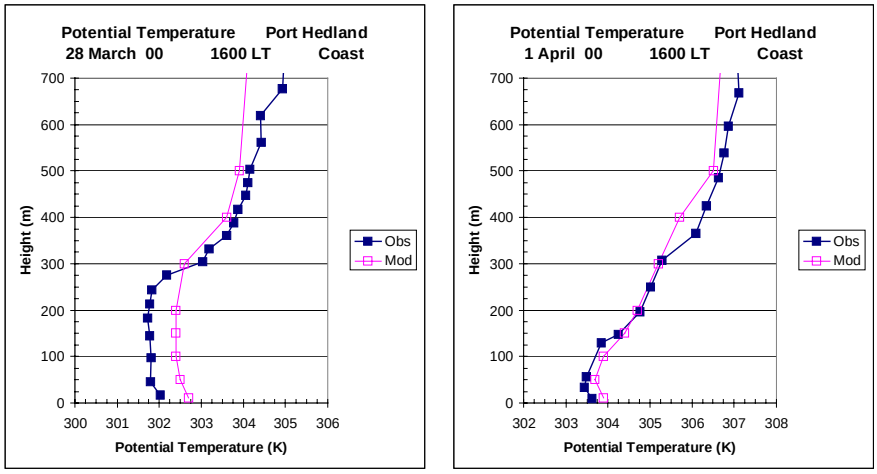

Figure 5.11. Observed (■) and TAPM modelled (□) potential temperature profiles at 1600 LT from a coastline site on 28 March 2000 and 1 April at Port Hedland.

Figure 5.12 shows the observed and modelled profiles on the same two days at a site 7 km inland. On 28 March, the mixed layer has grown from 250 m at the coast to a height of 400 m, and this has been simulated well by TAPM. Mixed-layer growth was more rapid on 1 April, as the growing layer was pushing into a less-stable layer on this day than on 28 March, with a height of 350 m reached at this inland station. The TAPM simulation showed good agreement.

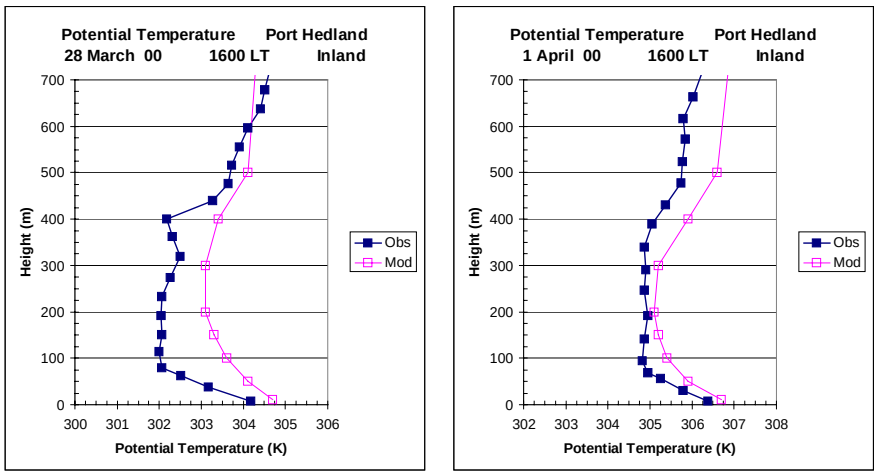

Figure 5.12. Observed (■) and TAPM modelled (□) potential temperature profiles at 1600 LT from a site 7 km inland on 28 March 2000 and 1 April at Port Hedland.

6 International model inter-comparison datasets

In 1991, The Joint Research Centre of the European Commission launched an initiative for increased cooperation and standardisation of atmospheric dispersion models for regulatory purposes. As part of the initiative, a series of conferences on “Harmonisation within Atmospheric Dispersion Modelling for Regulatory Purposes” was organised to promote the use of new-generation models within atmospheric dispersion modelling, and in general improve "modelling culture" (for more details see Olesen, 1995). A set of four short-range field data sets, called the Model Validation Kit, was prepared to facilitate a standard and uniform comparison of model results. The two most comprehensive of the four field datasets on point-source plume dispersion are the 1980–81 Kincaid (rural) dataset, and the 1985 Indianapolis (urban) dataset, both taken in the US and widely used for model evaluation purposes. These two datasets were taken in relatively simple orography (i.e. flat terrain, no coastal influences), where simple plume models should be expected to perform well. In contrast, TAPM can handle both simple and complex terrain cases through its 3-D prognostic meteorological component coupled with a detailed dispersion scheme. In Luhar and Hurley (2002a), TAPM is evaluated using the 1995 Kwinana (Australia) coastal dispersion data set involving meteorological, surface concentration and lidar plume moment data, and the results show that TAPM performs well in simulating coastal effects, such as sea breezes, fumigation and wind-direction shear.

In this Section, the performance of TAPM is evaluated for the Kincaid and Indianapolis datasets. The results are also compared with those from other commonly used models (i.e. ADMS3, AERMOD and ISCST3) that have also been applied to these datasets using observed meteorological, stability and turbulence data as inputs. TAPM was run with and without wind data assimilation (Luhar and Hurley, 2002a, 2002b), but in the summary presented here, only TAPM results for the simulations with wind data assimilation are shown. TAPM performed slightly worse without wind data assimilation, but results still compared well with the observations.

Since the above two data sets precede the global synoptic meteorological data supplied with TAPM, which are given from 1997, we used the National Center for Environmental Prediction (NCEP)/National Center for Atmospheric Research (NCAR) reanalysis data (Kalnay 1996) on horizontal wind components, temperature and moisture, to obtain the required synoptic fields in the model. These data have a horizontal resolution of 2.5º and a temporal resolution of 6 h, while the vertical levels are in a pressure coordinate system with the lowest five levels being 1000, 925, 850, 700 and 600 hPa.

6.1 Kincaid

EPRI’s (Electric Power Research Institute) Kincaid field study was conducted in 1980 and 1981 (Bowne et al., 1983). It involved sulfur hexafluoride (SF_6) tracer releases from the 187 m stack (with diameter 9 m) at the Kincaid power plant in Illinois, USA (89.49ºW, 39.59ºN). The power plant is surrounding by relatively flat farmland with some lakes (roughness length of about 0.1 m).

Most meteorological measurements were taken from 10-m and 100-m towers located on a central site about 650 m east of the power plant together with solar and terrestrial radiation measurement gear. The wind observations were taken at the 10, 30, 50 and 100 m AGL levels, while the temperature measurements were taken at the 10, 50 and 100 m levels. There are also data from a National Weather Service station 30.6 km northwest of the source, and profiles from routine radiosonde releases 120 km north of the source.

Hourly-averaged concentrations of SF_6 due to buoyant power station plumes were observed by ground-level monitors on a maximum of 12 arcs at distances 0.5, 1, 2, 3, 5, 7, 10, 15, 20, 30, 40 and 50 km from the stack. There are three measurement periods: 20 April–9 May 1980, 10–25 July 1980, and 16 May–1 June 1981. Figure 6.1 shows the locations of the stack, meteorological sites and the tracer monitors on 22 May 1981. A total of 171 hours of tracer data are available in the Model Validation Kit, representing mostly daytime convective cases. Arc-wise maxima were calculated from the crosswind concentration variation, and a quality indicator was assigned to each value. It is recommended that only the data with quality indicator 2 (maxima identified) and 3 (maxima well defined) be used for model comparison. Out of a total of 1284 arc-hours of data, 585 are quality 2 and 3, and 338 are quality 3.

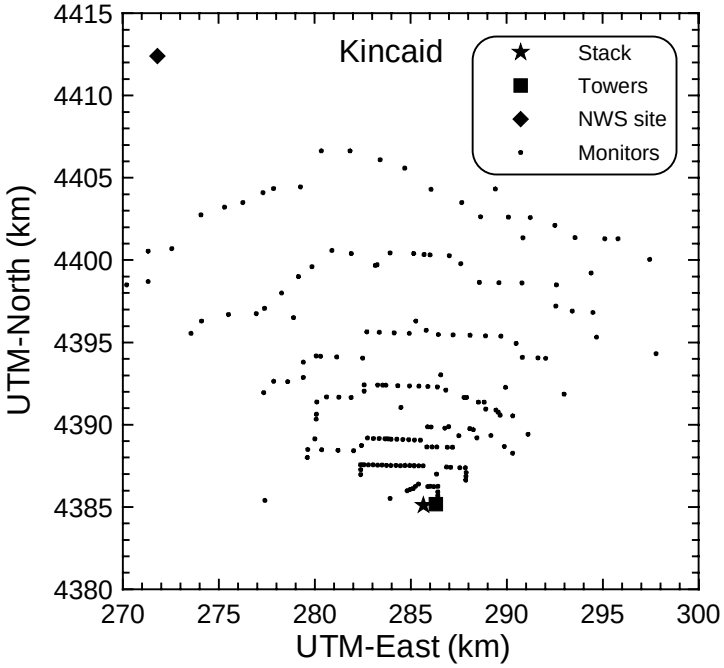

Figure 6.1. Concentration monitors (22 May 1981), and meteorological sites for the Kincaid study.

TAPM V2.0 was run for the above three data periods separately with an extra spin-up day at the start in each run. Three nested domains of 31 × 31 horizontal grid points at 16-km, 4-km, and 1-km spacing for the meteorology, and 61 × 61 horizontal grid points at 8-km, 2-km, and 0.5-km spacing for the pollution, both centred on the stack coordinates, were used. There were 25 vertical levels: 10, 25, 50, 100, 150, 200, 250, 300, 400, 500, 600, 750, 1000, 1250, 1500, 1750, 2000, 2500, 3000, 3500, 4000, 5000, 6000, 7000 and 8000 m. The model was run in Lagrangian mode to capture the near-source dispersion more accurately. For Kincaid data, a value of 0.5 is recommended for the moisture availability factor, which is defined as the ratio of the surface latent heat flux to the total surface heat flux. To match this value, we used deep soil moisture content of 0.15 kg kg^{-1}, which is also the model default value. The wind speeds and directions observed at the tower site at four levels, namely 10, 30, 50 and 100 m AGL, were assimilated in model calculations. The hourly average pollution predictions on the 0.5 km spaced grid were processed to obtain ground-level concentration maxima at the 0.5, 1, 2, 3, 5, 7, 10 and 15 km arcs while those on the 2-km spaced pollution grid were processed to obtain the maxima at the 20, 30, 40 and 50 km arcs.

Tables 6.1 and 6.2 give model performance statistics recommended by the Model Validation Kit, for TAPM. Also given are these statistics, reported in McHugh *et al.* (1999), for the regulatory models ISCST3 (USA), AERMOD (USA) and ADMS3 (UK). It is clear that the observations are best predicted by ADMS3 and TAPM, with AERMOD and ISCST3 worse for all statistics. For Quality 3 data, the correlation coefficient is the highest for TAPM, followed closely by ADMS3, and then AERMOD and ISCST3, while the factor-of-two (fraction of predictions within a factor of two of observations) measure shows that ADMS3 performs the best, closely followed by TAPM, and then AERMOD and ISCST3.

Table 6.1. Model performance statistics for Kincaid, Quality 2&3 data.

Model	MEAN	STD	BIAS	NMSE	CORR	FAC2	FB	FS
C_OBS	41.0	39.3	0.0	0.00	1.00	1.00	0.00	0.00
ISCST3	23.1	53.3	17.9	3.8	0.26	0.26	0.56	-0.30
AERMOD	20.3	24.1	20.7	2.3	0.35	0.33	0.68	0.48
ADMS3	43.2	33.5	-2.2	0.8	0.49	0.58	-0.05	0.16
TAPM	60.4	58.6	-19.4	1.3	0.44	0.50	-0.38	-0.40

MEAN = Arithmetic Mean (ng m^{-3} (g s^{-1})$^{-1}$), STD = Standard Deviation (ng m^{-3} (g s^{-1})$^{-1}$), BIAS = Difference between Observed and Predicted Mean (ng m^{-3} (g s^{-1})$^{-1}$), NMSE = normalised mean square error, Corr = correlation coefficient, Fac2 = factor of two, Fb = normalised bias, Fs = normalised sigma.

Table 6.2. Model performance statistics for Kincaid, Quality 3 data.

Model	MEAN	STD	BIAS	NMSE	CORR	FAC2	FB	FS
C_OBS	54.3	40.3	0.0	0.0	1.00	1.00	0.00	0.00
ISCST3	30.0	60.0	24.3	2.8	0.26	0.28	0.58	-0.39
AERMOD	21.8	21.8	32.6	2.1	0.40	0.29	0.86	0.59
ADMS3	51.7	34.7	2.7	0.6	0.45	0.67	0.05	0.15
TAPM	67.4	59.8	-13.0	0.8	0.48	0.55	-0.24	-0.39

MEAN = Arithmetic Mean (ng m^{-3} (g s^{-1})$^{-1}$), STD = Standard Deviation (ng m^{-3} (g s^{-1})$^{-1}$), BIAS = Difference between Observed and Predicted Mean (ng m^{-3} (g s^{-1})$^{-1}$), NMSE = normalised mean square error, Corr = correlation coefficient, Fac2 = factor of two, Fb = normalised bias, Fs = normalised sigma.

Table 6.3 shows ratios (predicted/observed) of average (MEAN), Robust Highest Concentration (RHC – see Appendix for definition) and maximum concentration (MAX) for Kincaid Quality 2&3 data (extreme concentrations for the other models were taken from Hanna *et al*., 1999). The ratios of the MEAN reiterate the results described above, while the RHC and MAX ratios emphasise the performance of the models near the extreme end of the concentration distribution, which is very important for regulatory applications. The results show that TAPM performs well for prediction of extreme concentrations with an over-prediction of about 20%. In contrast, ISCST3 and AERMOD under-predict by almost a factor of two, and ADMS3 also under-predicts, but by not quite as much as ISCST3 and AERMOD. Figure 6.2 shows TAPM Quantile-Quantile (Q-Q) plots of the (sorted) predicted versus the

(sorted) observed concentrations for both Quality 2&3 and Quality 3 data. These plots again illustrate that TAPM tends towards a slight over-prediction for all concentration levels.

Table 6.3. Model performance ratios (Predicted/Observed) for Kincaid, Quality 2&3 data (and for Quality 3 data for the MEAN).

Model	MEAN_RATIO	RHC_RATIO	MAX_RATIO
ISCST3	0.56 (0.55)	0.61	0.55
AERMOD	0.50 (0.40)	0.52	0.48
ADMS3	1.05 (0.95)	0.70	0.66
TAPM	1.47 (1.24)	1.18	1.20

MEAN_RATIO = Ratio (Predicted/Observed) of Arithmetic Mean Concentration,
RHC_RATIO = Ratio (Predicted/Observed) of Robust Highest Concentration (RHC),
MAX_RATIO = Ratio (Predicted/Observed) of Maximum Concentration.
Note that a ratio of 1.0 is perfect, and a value between 0.5 and 2.0 is within a factor of 2.

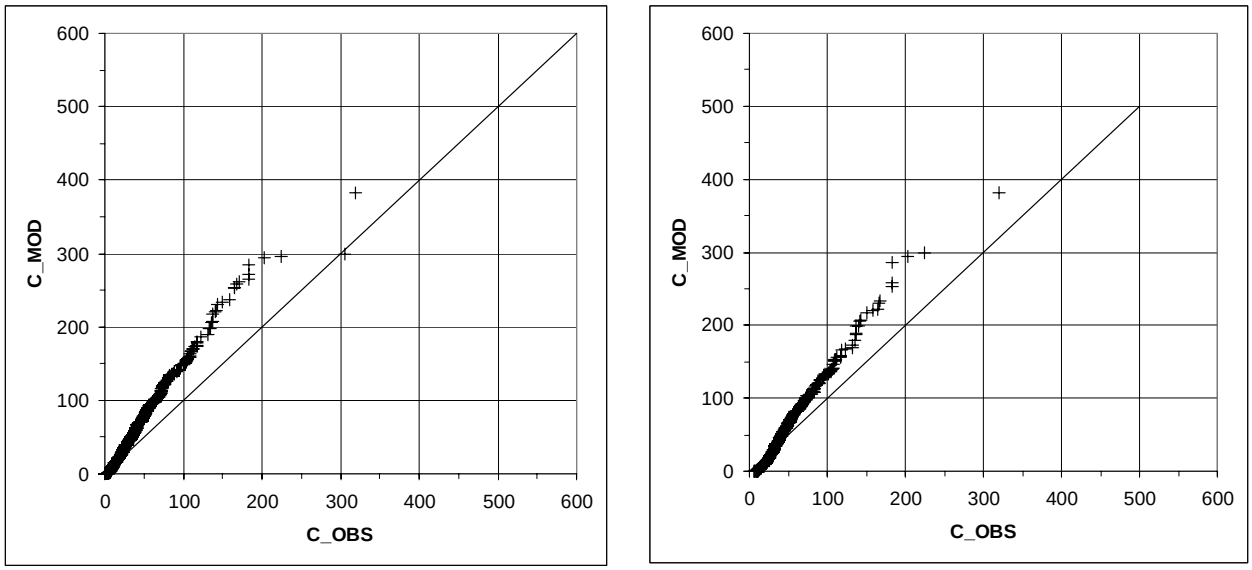

Figure 6.2. Kincaid Quantile-Quantile plots for Quality 2&3 (left) and Quality 3 (right) data.

In summary, the results show that for the Kincaid dataset

- TAPM performs well for both the mean and for the extreme performance statistics,
- ADMS3 performs well for the mean but not as good for the extreme performance statistics,
- AERMOD performs poorly for both the mean and the extreme performance statistics,
- ISCST3 performs poorly for both the mean and the extreme performance statistics.

with TAPM performing the best overall.

6.2 Indianapolis

A full description of EPRI's Indianapolis field study, conducted during 16 September to 12 October, 1985, is given in TRC (1986). It involved SF_6 tracer releases from the 83.8-m

stack (with diameter 4.72 m) at the Perry K power plant on the southwest edge of Indianapolis, Indiana, USA (86°12′W, 39°48′N). The stack is located in a typical industrial/commercial/urban complex with many buildings within one or two kilometres (roughness length of about 1 m), and relatively flat local terrain.

Meteorological observations were taken from a 94 m height at the top of a bank building in the middle of the urban area, from two 10-m towers in suburban and rural areas, and an 11-m tower at an urban location. In addition, vertical meteorological profiles were also taken. Hourly-averaged concentrations were observed on a network of up to 160 ground-level monitors on 12 arcs at distances 0.25, 0.5, 0.75, 1.0, 1.5, 2, 3, 4, 6, 8, 10 and 12 km from the stack. To sample the plume, the network of monitors was moved so that it was downwind of the source. Data were taken in 8 or 9 hour test blocks with 19 such blocks altogether. Figure 6.3 shows the locations of the stack, meteorological sites and the tracer monitors corresponding to the test block 9. A total of 170 hours of tracer data is available, representing all stability classes and most wind speed ranges. Arc-wise maxima were calculated from the crosswind concentration variation, and a quality indicator was assigned to each value. It is recommended that only the data with quality indicator 2 (maxima identified) and 3 (maxima well defined) be used for model comparison. Out of a total of 1511 arc-hours of data, 1216 are quality 2 and 3, and 469 are quality 3.

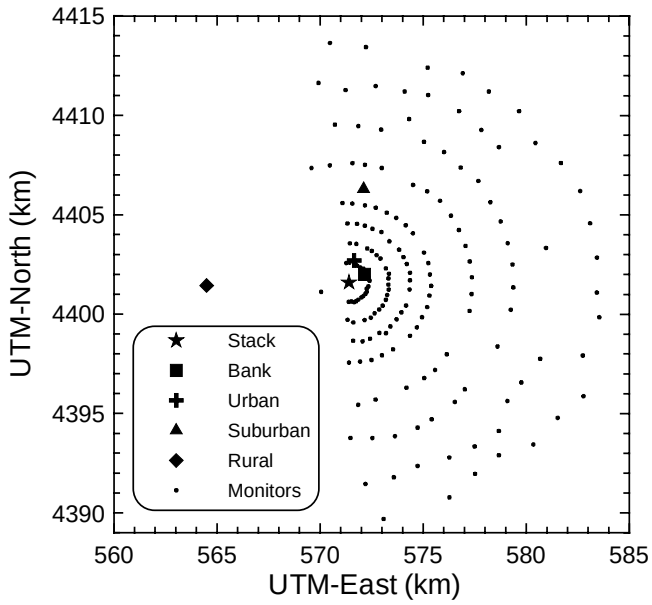

Figure 6.3. Tracer monitors (Test 9), and meteorological sites for the Indianapolis study.

TAPM was run for the period 15 September to 12 October, 1985, with four nested domains of 30×30 horizontal grid points at 30-km, 10-km, 3-km and 1-km spacing for the meteorology, and 101×101 horizontal grid points at 7.5-km, 2.5-km, 0.75-km and 0.25-km spacing for the pollution, both centred on the stack coordinates. There vertical levels were the same as in the Kincaid case. The model was run in Lagrangian mode to capture the near-source dispersion more accurately. For Indianapolis data, a value of 0.5 is recommended for the moisture availability factor, which is defined as the ratio of the surface latent heat flux to the total surface heat flux. To match this value, we used a deep soil moisture content of 0.3 kg kg^{-1}, which was different to that used for Kincaid, as the dominant land use here was urban rather

than grassland. The wind speeds and directions observed at the Urban tower (10 m AGL) and the Bank building (94 m) were assimilated into model calculations. The hourly average pollution predictions on the 0.25-km spaced grid were processed to obtain ground-level concentration maxima at the 12 arcs.

Tables 6.4 and 6.5 give model performance statistics recommended by the Model Validation Kit, for TAPM. Also given are these statistics, reported in McHugh *et al.* (1999) and CERC (1999), for the regulatory models ISCST3 (USA), AERMOD (USA) and ADMS3 (UK). All models do a good job for the performance statistics, although ISCST3 tends to over-predict the mean for Quality 2&3 data, and TAPM has by far the best correlation coefficient. For the factor-of-two measure, ISCST3 performs best, while it is a little lower for TAPM than for any other model. This is mostly because in TAPM occasionally the plume does not mix down to the ground under night-time stable conditions, while the observations show otherwise. In all other models, *observed* meteorological, stability and turbulence data are used as inputs with the assumption that the minimum value of the Monin-Obukhov length is 50 m during stable conditions, which moderates the stability (to account for urban effects) and causes the plume to diffuse more and reach the ground. Overall, AERMOD performs better than ISCST3, but the two top performing models are TAPM and ADMS3.

Table 6.4. Model performance statistics for Indianapolis, Quality 2&3.

Model	MEAN	STD	BIAS	NMSE	CORR	FAC2	FB	FS
C_OBS	258	222	0.0	0.0	1.00	1.00	0.00	0.00
ISCST3	404	321	-146	1.4	0.16	0.45	-0.44	-0.37
AERMOD	225	196	33	1.3	0.17	0.41	0.14	0.13
ADMS3	265	255	-8	1.3	0.26	0.42	-0.03	-0.14
TAPM	248	284	10	1.0	0.51	0.36	0.04	-0.25

MEAN = Arithmetic Mean (ng m^{-3} (g s^{-1})$^{-1}$), STD = Standard Deviation (ng m^{-3} (g s^{-1})$^{-1}$), BIAS = Difference between Observed and Predicted Mean (ng m^{-3} (g s^{-1})$^{-1}$), NMSE = normalised mean square error, Corr = correlation coefficient, Fac2 = factor of two, Fb = normalised bias, Fs = normalised sigma.

Table 6.5. Model performance statistics for Indianapolis, Quality 3.

Model	MEAN	STD	BIAS	NMSE	CORR	FAC2	FB	FS
C_OBS	352	221	0.0	0.0	1.00	1.00	0.00	0.00
ISCST3	418	239	-66	0.6	0.17	0.61	-0.17	-0.08
AERMOD	269	199	83	0.8	0.20	0.53	0.27	0.11
ADMS3	350	266	2	0.8	0.22	0.52	0.01	-0.18
TAPM	376	316	-25	0.7	0.45	0.46	-0.07	-0.35

MEAN = Arithmetic Mean (ng m^{-3} (g s^{-1})$^{-1}$), STD = Standard Deviation (ng m^{-3} (g s^{-1})$^{-1}$), BIAS = Difference between Observed and Predicted Mean (ng m^{-3} (g s^{-1})$^{-1}$), NMSE = normalised mean square error, Corr = correlation coefficient, Fac2 = factor of two, Fb = normalised bias, Fs = normalised sigma.

Table 6.6 shows ratios (predicted/observed) of average (MEAN), Robust Highest Concentration (RHC) and maximum concentration (MAX) for Indianapolis Quality 2&3 data

(extreme concentrations for the other models were taken from Hanna *et al*., 1999). The ratios of the MEAN reiterate the results described above, while the RHC and MAX ratios emphasise the performance of the models near the extreme end of the concentration distribution. The results show that TAPM and ADMS3 perform very well for prediction of extreme concentrations, and that AERMOD and ISCST3 also perform well, with a tendency for some underestimation for AERMOD and over-estimation for ISCST3. Figure 6.4 shows TAPM Quantile-Quantile (Q-Q) plots of the (sorted) predicted versus the (sorted) observed concentrations for both Quality 2&3 and Quality 3 data. These plots again illustrate that TAPM tends towards a very slight over-prediction for all concentration levels, except at the very low concentration end of the distribution.

Table 6.6. Model performance ratios (Predicted/Observed) for Indianapolis, Quality 2&3 data (and for Quality 3 data for the MEAN).

Model	MEAN_RATIO	RHC_RATIO	MAX_RATIO
ISCST3	1.57 (1.19)	1.14	1.26
AERMOD	0.87 (0.76)	0.86	1.13
ADMS3	1.03 (0.99)	1.03	1.07
TAPM	0.96 (1.16)	0.92	1.00

MEAN_RATIO = Ratio (Predicted/Observed) of Arithmetic Mean Concentration,
RHC_RATIO = Ratio (Predicted/Observed) of Robust Highest Concentration (RHC),
MAX_RATIO = Ratio (Predicted/Observed) of Maximum Concentration.
Note that a ratio of 1.0 is perfect, and a value between 0.5 and 2.0 is within a factor of 2.

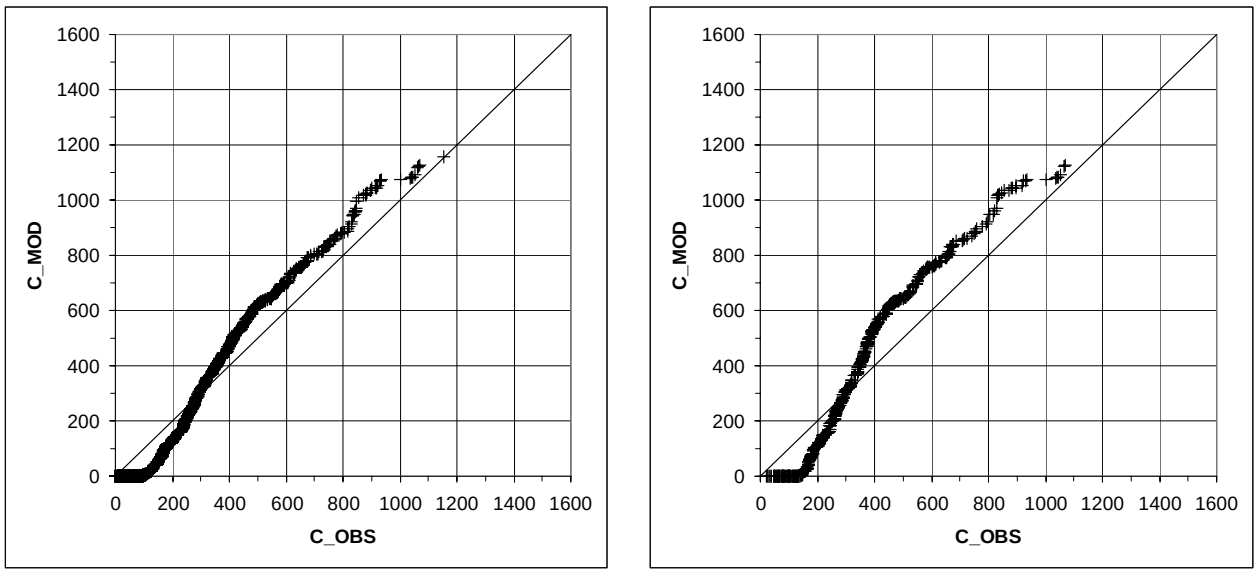

Figure 6.4. Indianapolis Quantile-Quantile plots for Quality 2&3 (left) and Quality 3 (right) data.

In summary, the results show that for the Indianapolis dataset, all models do a reasonable job for mean and extreme performance statistics, with little bias shown by TAPM and ADMS3, some under-prediction shown by AERMOD, some over-prediction shown by ISCST3, and with TAPM performing the best overall.

7 Point source building wake dispersion in the wind tunnel

The effect of building wakes on plume rise and dispersion in TAPM is based on the Plume Rise Model Enhancements (PRIME) approach of Schulman *et al*. (2000). The PRIME model uses an along-wind coordinate system, and so first each building is transformed to be in this system. Effective building dimensions and cavity and wake dimensions are then calculated for each building, which are used to determine the combined wake meteorology and turbulence. Plume rise is affected by the modified meteorology and turbulence for point sources in both EGM and LPM modes, while dispersion is influenced only for plumes in LPM mode. LPM calculations are done for both the cavity and wake regions, rather than specifying a uniform concentration in the cavity as is done in PRIME.

In this Section, TAPM is used in LPM mode to simulate point source dispersion in a single building wake for the wind tunnel experiments of Thompson (1993). These data provide an independent test of the building wake algorithms, as they have not been used in the development of PRIME, and represent point source dispersion for non-buoyant sources in the near-wake or cavity region for four different building shapes. Schulman *et al*. (2000) also used PRIME and ISC3 to simulate one of the building shapes used by Thompson (1993), while the equation for maximum (uniform) cavity concentration for both of these models has been used here for the remaining building shapes. The model was run with flat terrain in a nested, non-time varying synoptic mode, assimilating a uniform wind speed profile over the lowest 300 m, with a pollution inner grid spacing of 50 m. The dimensions of the four buildings used were:

- BLD1: $W = H$ and $L = H$;
- BLD2: $W = 2H$ and $L = H$;
- BLD3: $W = 4H$ and $L = H$;
- BLD4: $W = H$ and $L = 2H$;

where W = building width, L = building length, H = building height, and here we have used H = 100 m. The stack height for the point source was $H_S = 0.5H$, located at one stack height downwind of the centre of the lee face of the building (i.e., at downwind distance $X = H$, and crosswind distance $Y = 0$).

Non-dimensional plume centreline ground level concentrations as a function of downwind distance are shown in Figure 7.1 for both observations and model predictions for BLD1 (observations, and predictions by both PRIME and ISC3, are taken from Schulman *et al*., 2000). The results show that TAPM predicts the maximum cavity concentration very well, but tends to underestimate the concentration behind the source (between the building and the stack), while PRIME underestimates the maximum, but represents the concentration behind the source well, and ISC3 significantly underestimates the cavity concentration. All models do a good job in the far-wake region from about $X = 4H$ onwards.

The maximum cavity concentrations have also been calculated for all models for each of the four building shapes and the results are shown in Figure 7.2. The results show that TAPM performs well in representing both the magnitude and the variation of the maximum cavity concentration with building shape. PRIME also does a good job for BLD3 and BLD4, but tends to underestimate the maximum cavity concentration for BLD1 and particularly for BLD2. ISC3 has a similar variation of maximum cavity concentration as for PRIME, but the magnitude is much too low.

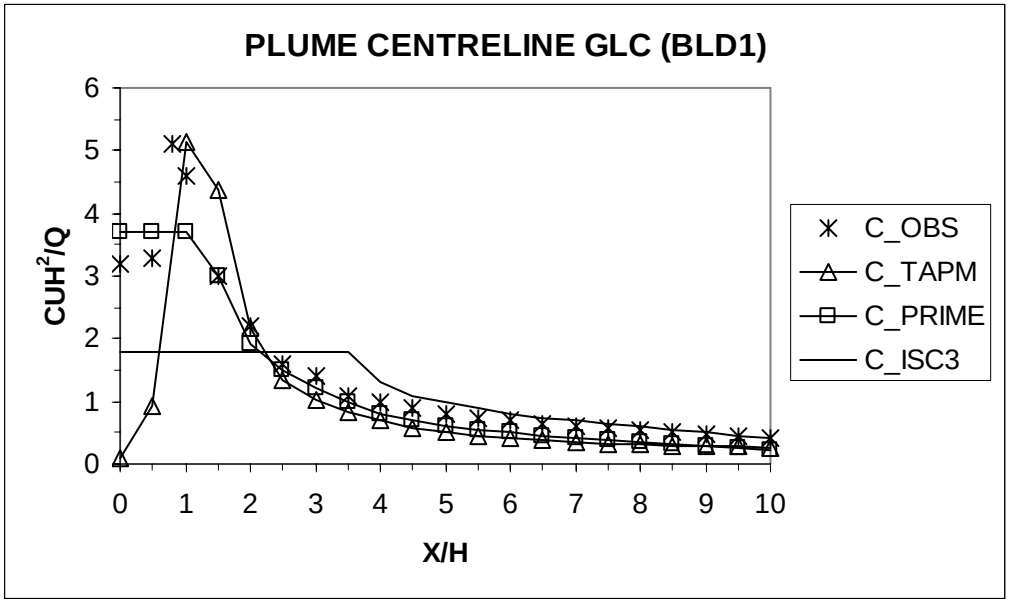

Figure 7.1. Observed (OBS) and predicted (TAPM, PRIME and ISC3) plume centreline ground level concentration (GLC), downwind of BLD1.

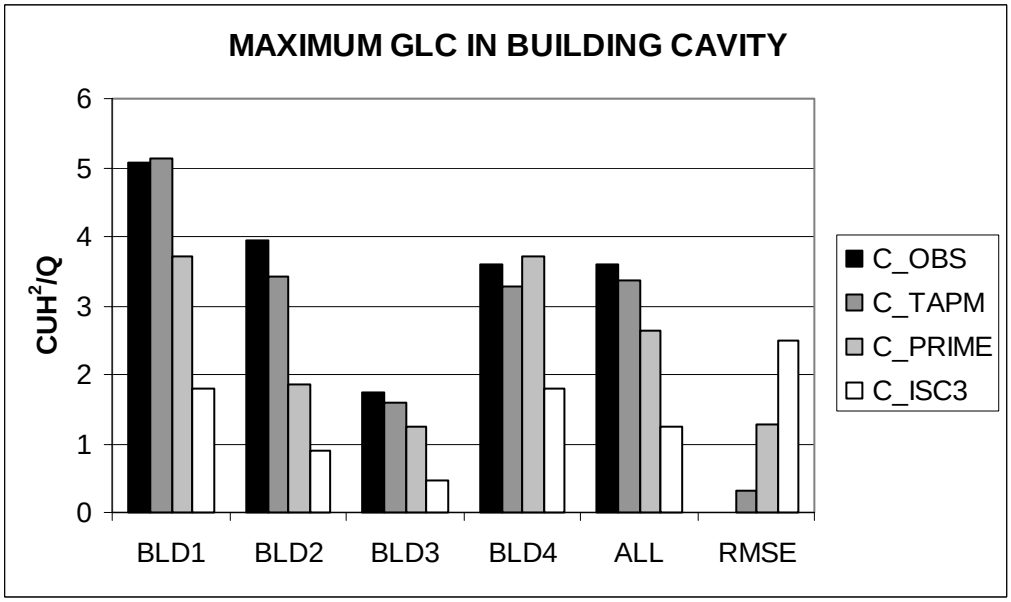

Figure 7.2. Observed (OBS) and predicted (TAPM, PRIME and ISC3) maximum plume centreline ground level concentration (GLC), for BLD1, BLD2, BLD3, BLD4, and the average (ALL) and root mean square error (RMSE) over all buildings.

In summary, these results show that TAPM is performing well for both near- and far-wake regions for various building shapes, and that in particular, TAPM represents the maximum downwind concentration from these independent wind-tunnel experiments very well, while also performing well (as do both PRIME and ISC3) in the far-wake region. It is expected that TAPM will perform in a similar manner to PRIME for buoyant plumes outside of the cavity region, as for this situation the algorithms in TAPM for plume rise and wake meteorology and turbulence are similar to those in PRIME.

Acknowledgments

Thanks to:

- US Geological Survey, Earth Resources Observation Systems (EROS) Data Center Distributed Active Archive Center (EDC DAAC), for access to the global terrain and land-use datasets;
- Geoscience Australia and CSIRO Wildlife and Ecology for access to the Australian terrain and land-use datasets;
- Australian Bureau of Meteorology for the LAPS/GASP synoptic meteorology datasets;
- National Centers for Environmental Prediction (NCEP)/National Center for Atmospheric Research (NCAR) for access to the synoptic reanalysis data used for the Kincaid and Indianapolis tracer studies, and to Mark Collier and Mary Edwards for processing this data into a form suitable for use by TAPM;
- US National Center for Atmospheric Research (NCAR) for access to the global sea-surface temperature dataset;
- Brian Weymouth for providing Cape Grim meteorological data, and to the Cape Grim Baseline Air Pollution Station and Arthur Downey of the Australian Bureau of Meteorology;
- EPA Victoria for allowing access to the Melbourne emissions inventory and for providing meteorology and air pollution data from their air monitoring network;
- Department of Environmental Protection (DEPWA) for access to the Kwinana, Perth and Pilbara emissions data and air monitoring data;
- those organisations involved with developing the Kincaid and Indianapolis tracer datasets in the Model Validation Kit, as part of the European initiative on “Harmonisation within Atmospheric Dispersion Modelling for Regulatory Purposes”.

References

Baines, P.G., and Murray, D. (1991). 'Modelling of the airflow over Cape Grim', *Baseline 91*, 20-24.

Bowne N. E., Londergan R. J., Murray D. R. and Borenstein H. S. (1983). 'Overview, results and conclusions for the EPRI plume model validation project: plain site', EPRI Report EA-3074, EPRI, Palo Alto, CA 94304.

Cox W. and Tikvart J. (1990). 'A statistical procedure for determining the best performing air quality simulation.' *Atmos. Environ*., **24A**, 2387-2395.

CERC (1999). 'ADMS3 Validation Summary', Cambridge Environmental Research Consultants, Cambridge, UK, 16 pp.

Hanna S. (1989). 'Confidence limits for air quality model evaluations, as estimated by bootstrap and jackknife resampling methods.' *Atmos. Environ*., **23**, 1385-1398.

Hanna S., Egan B., Purdum J., and Wagler J. (1999). 'Evaluation of ISC3, AERMOD and ADMS dispersion models with observations from five field sites.' HC Report P020, API, 1220 L St. NW, Washington, DC 20005-4070.

Hamilton, S. (1999). 'A comparison of the air dispersion models AUSPLUME and AUSPUFF', *Clean Air*, **33**, 44-49.

Hurley P. (1999). 'The Air Pollution Model (TAPM) Version 1. Technical Description and examples', CSIRO Atmospheric Research Technical Paper No. 43. 41 pp.

Hurley P. (2000). 'Verification of TAPM meteorological predictions in the Melbourne region for a winter and summer month.' *Aust. Met. Mag*., **49**, 97-107.

Hurley P. (2002). 'The Air Pollution Model (TAPM) Version 2. Part 1: Technical Description', CSIRO Atmospheric Research Technical Paper No. 55. 49 pp.

Hurley P., Blockley A., and Rayner K. (2001). 'Verification of a prognostic meteorological and air pollution model for year-long predictions in the Kwinana region of Western Australia.' *Atmos. Environ*., **35**, 1871-1880.

Hurley P. and Luhar A. (2000). 'The Kwinana Coastal Fumigation Study: Meteorological and turbulence modelling on selected days.' *Boundary-Layer Meteorol.*, **94**, 115-138.

Hurley, P., Manins P., Lee S., Boyle R., Ng. Y. and Dewundege P. (2002), 'Year-long urban airshed modelling in Melbourne: Verification of TAPM for photochemical smog and particles', *Submitted to the 16th International Clean Air and Environment Conference, Christchurch, New Zealand, 18-22 August 2002*.

Johnson, G.M., Quigley, S.M. and Smith, J.G. (1990). 'Management of photochemical smog using the airtrak approach', *Proceedings of the 10th International Conference of the Clean Air Society of Australia and New Zealand, Auckland, New Zealand, March 1990*.

Kalnay E. et al. (1996). 'The NCEP/NCAR 40-Year Reanalysis Project', *Bull. Amer. Meteorol. Soc.*, **77**, 437–71.

Lorimer, G. (1986). 'The AUSPLUME Gaussian plume dispersion model', Environment Protection Authority of Victoria, publication No. 264.

Luhar A. and Hurley P. (2002a). 'Evaluation of TAPM using the Indianapolis (urban) and Kwinana (coastal) field data sets', *Submitted to the 16th International Clean Air and Environment Conference*, Christchurch, New Zealand, 18-22 August.

Luhar A. and Hurley P. (2002b). 'Comparison of meteorological and dispersion predictions obtained using TAPM with the Indianapolis (urban), Kincaid (rural) and Kwinana (coastal) field data sets', *Submitted to the 8th International Conference on Harmonisation within Atmospheric Dispersion Modelling for Regulatory Purposes,* Sofia, Bulgaria, 14–17 October.

McHugh C. A., Carruthers D. J., Higson, H. & Dyster S. J. (1999). 'Comparison of model evaluation methodologies with application to ADMS3 and US models', *Proceedings of the 6th International Conference on Harmonisation within Atmospheric Dispersion Modelling for Regulatory Purposes,* Rouen, France, 11–14 October.

Ng Y.L. and Boyle R. (2002). 'Emission Projections for the Melbourne Air Quality Improvement Plan', *Submitted to the 16th International Clean Air and Environment Conference, Christchurch, New Zealand, 18-22 August 2002*.

Ng Y.L. and Wong N. (2002). 'Preparing Emissions Inventory Data for the Australian Air Quality Forecasting System', *Submitted to the 16th International Clean Air and Environment Conference, Christchurch, New Zealand, 18-22 August 2002.*

Olesen H. R. (1995). 'The model validation exercise at Mol: overview of results', *Int. J. Environ. Pollut.* **5**, 761–84.

Pielke R.A. (1984). 'Mesoscale Meteorological modelling', Academic Press, Orlando, 612 pp.

Physick W.L. (2001). 'Meteorology and air quality of the Pilbara region. CSIRO Division of Atmospheric Research. A Report to Department of Environmental Protection, W.A. 69 pp. May 2001.

Physick W.L. and Blockley A. (2001). 'An evaluation of air quality models for the Pilbara region', CSIRO Division of Atmospheric Research. A Report to the Department of Environmental Protection, Western Australia, 98 pp, June 2001.

Physick W.L., Blockley A., Farrar D., Rayner K. and Mountford P. (2002b). 'Application of three air quality models in the Pilbara region', *Proceedings of the 16th International Clean Air and Environment Conference, Christchurch, New Zealand, August 2002.*

Physick W.L. and Cope M.E. (2001). 'A screening procedure for monitoring ozone and nitrogen dioxide in "small- to medium-sized" cities: Phase I – validation of the procedure', CSIRO Division of Atmospheric Research. A Report to the air quality NEPM standards Peer Review Committee, Environment Australia.

Physick W.L., Cope M.E. and Stuart A. (2002a). 'Evaluation of a population-surrogate emissions inventory for Perth using TAPM', *Proceedings of the 16th International Clean Air and Environment Conference, Christchurch, New Zealand, August 2002.*

Physick W.L., Rayner K. and Mountford P. (2000). 'Dispersion meteorology of the Pilbara region', *Proceedings of the 15th International Clean Air and Environment Conference, Sydney, Australia, November 2000.*

Puri K., Dietachmayer G.S., Mills G.A., Davidson N.E., Bowen R.A., and Logan L.W. (1998). 'The BMRC Limited Area Prediction System, LAPS', *Australian Meteorol. Mag.*, **47**, 203-223.

Rayner K. (1998). 'A model-based sulfur dioxide control policy for the Kwinana industrial region', *Proceedings of the 11th Clean Air and Environment Conference, Durban, South Africa, 13-18 September, 1998.*

Rayner K. (2000). 'Improvements in the coastal dispersion model DISPMOD', *Proceedings of the 15th International Clean Air and Environment Conference, Sydney, Australia, 26-30 November 2000*.

Schulman L., Strimaitis D. and Scire J. (2000). 'Development and evaluation of the PRIME plume rise and building downwash model', *J. Air & Waste Manage. Assoc.*, **50**, 378-390.

Thompson R. (1993). 'Building Amplification factors for sources near buildings: A wind-tunnel study', *Atmos. Environ.*, **27A**, 2313-2325.

TRC (1986). Urban Power Plant Plume Studies, EPRI Report EA-5468, EPRI, 3412 Hillview Ave, Palo Alto, CA 94304.

Willmott C.J. (1981). 'On the Validation of Models', *Phys. Geography*, **2**, 184-194.

APPENDIX

The statistics used to measure meteorological model performance in this paper are based on those used by Willmott (1981) and Pielke (1984), as described below.

Predicted Mean $P_{mean} = \sum_{i=1}^{N} P_i$, where P_i are the predictions.

Observed Mean $O_{mean} = \sum_{i=1}^{N} O_i$, where O_i are the observations.

Predicted Standard Deviation $P_{std} = \sqrt{\frac{1}{N-1}\sum_{i=1}^{N}\left(P_i - P_{mean}\right)^2}$.

Observed Standard Deviation $O_{std} = \sqrt{\frac{1}{N-1}\sum_{i=1}^{N}\left(O_i - O_{mean}\right)^2}$.

Pearson Correlation Coefficient $r = \frac{N\left(\sum_{i=1}^{N} O_i P_i\right) - \left(\sum_{i=1}^{N} O_i\right)\left(\sum_{i=1}^{N} P_i\right)}{\sqrt{\left[N\left(\sum_{i=1}^{N} O_i^2\right) - \left(\sum_{i=1}^{N} O_i\right)^2\right]\left[N\left(\sum_{i=1}^{N} P_i^2\right) - \left(\sum_{i=1}^{N} P_i\right)^2\right]}}$.

Root Mean Square Error $RMSE = \sqrt{\frac{1}{N}\sum_{i=1}^{N}\left(P_i - O_i\right)^2}$.

Systematic Root Mean Square Error $RMSE_S = \sqrt{\frac{1}{N}\sum_{i=1}^{N}\left(\hat{P}_i - O_i\right)^2}$.

Unsystematic Root Mean Square Error $RMSE_U = \sqrt{\frac{1}{N}\sum_{i=1}^{N}\left(\hat{P}_i - P_i\right)^2}$.

Index of Agreement $IOA = 1 - \frac{\sum_{i=1}^{N}\left(P_i - O_i\right)^2}{\sum_{i=1}^{N}\left(\left|P_i - O_{mean}\right| + \left|O_i - O_{mean}\right|\right)^2}$.

Measures of Skill $SKILL_E = \frac{RMSE_U}{O_{std}}$, $SKILL_V = \frac{P_{std}}{O_{std}}$ and $SKILL_R = \frac{RMSE}{O_{std}}$.

Note that N is the number of observations and $\hat{P}_i = a + bO_i$ is the linear regression fitted formula with intercept (a) and slope (b).

The Robust Highest Concentration $RHC = C(R) + \left(\overline{C} - C(R)\right)\ln\left((3R-1)/2\right)$ pollution statistic is from Cox and Tikvart (1990), with $C(R)$ the R^{th} highest concentration and $\overline{C}$ the mean of the top R-1 concentrations. The value of R = 11 is used here so that $\overline{C}$ is the average of the top-ten concentrations, which is an accepted statistic for evaluation of model performance (Hanna, 1989). The RHC is preferred to the actual peak value because it mitigates the undesirable influence of unusual events, while still representing the magnitude of the maximum concentration (unlike percentiles or averages over the top-percentiles). The statistical performance measures used here for pollution with the Kincaid and Indianapolis datasets are the same as those used by Olesen (1995) in the Model Validation Kit.